SUPPORTING INFORMATION: EXTENDED RESULTS & DISCUSSION

EXTENDED RESULTS

Structural analysis

Fresh samples. The adult turkey beard was purchased as a dried specimen and the epidermis has a flaky appearance under microscopy (Fig. S1A, F). The bristles themselves also show a flaky appearance on their keratin surface when viewed in SEM under high magnification (Fig. S1B–C). Their cross sections show a solid, homogeneous structure and when cut, the bristles show fraying, splitting, and flaking at their ends (Fig. S1D–E).

The juvenile turkey beard shows similar features to the adult beard with a flaky or 'scaly' texture to the epidermis (Fig. S2A, F) and a flaky texture to the keratin of the bristles under higher magnification (Fig. S2B–C). The bristle cross sections also are homogenous and prone to splitting or fraying at their ends when cut (Fig. S2D–E). The variation in bristle cross-sectional shape is more apparent in the juvenile than the adult, with some bristles flattened compared to more rounded bristles.

The predominantly black crocodile scale shows a non-uniformly pigmented outer surface with a light colored, soft internal layer (Fig. S3A–B). The outer surface shows prominent flaking or cracking resulting in sub-polygonal flakes (Fig. S3C). At greater magnification, a rippled texture is apparent on the surface of the outer layer (Fig. S3D). A sharp contact can be observed between the outer and inner layers in cross section (Fig. S3E). The inner layer shows a more fibrous composition than the outer layer (Fig. S3F).

The predominantly white crocodile scale shows the same structure as the predominantly black scale. The outer surface is not uniformly pigmented (Fig. S4A), shows prominent flaking or cracking resulting in sub-polygonal flakes (Fig. S4B), and has a rippled pattern at higher magnification (Fig. S4C). There is a sharp contact between the outer and inner layers (Fig. S4D–E). The outer layer's cross section reveals that it is composed of multiple, overlapping keratinous sub-layers and even the deeper sub-layers show the rippled patterning on their surface (Fig. S4F).

The black feather has a white fringe (Fig. S5A). The rachis surface is simple but some topographic variability is apparent (i.e., it is not a completely smooth surface) (Fig. S5C). The calamus shows more complex keratin layering and folding than the rachis (Fig. S5D–E). The rachis cross section shows a central pith filled with medulloid cells and/or melanosomes and an outer cortex with a columnar pattern radiating outward (Fig. S5F).

The iridescent feather shows the most prominent iridescence at the distal portion of the vane (Fig. S6A). In the iridescent region, the barbules show a unique, broadened morphology (Fig. S6B). The plumulaceous barbules show evenly-spaced nodes (Fig. S6C). The rachis is relatively smooth but the calamus has more complex surface topology (Fig. S6D). The cross sections of the barbs show compartmentalization consisting of sub-polygonal medulloid cells (Fig. S6E). The rachis cross section has a central pith consisting of medulloid cells and/or melanosomes (Fig. S6F). However, the outer cortex is disorganized and does not show the columnar structure seen in the black feather, and the cross-sectional shape is overall more irregular.

The white feather (Fig. S7A) has pennaceous barbules that do not show the same proximal-distal variation seen in the black feather, but instead consist of the thickened ridge on

one side that supports a flattened vane (Fig. S7B). The plumulaceous barbules show evenly-spaced nodes (Fig. S7C). The rachis surface is not perfectly smooth, but is not relatively complex topographically (Fig. S7D–E). The rachis cross section shows an outer layer with columnar structuring and a small central pith consisting of medulloid cells (Fig. S7F).

The horse hair is darkly pigmented and coarse (Fig. S8A). The surface of the hair shows flaking in a manner reminiscent of the turkey beard bristles (Fig. S8B–D). The cross section is solid, but disorganized (Fig. S8E–F). The cut end of the strand did not split or fray like the turkey bristles did. The turkey bristles also show a more organized, almost concentric structuring of keratin in cross section compared to the more clumped appearance of the keratin in the hair.

The avian reticulate scales are sub-polygonal, with distinct boundaries between each scale (Fig. S9A–B). The surface of the outer layer is rough, reminiscent to the surface of the outer layer of crocodile scales (Fig. S9C) and at higher magnification it appears topographically complex (Fig. S9D). The cross section shows a fairly well defined contact between an inner and outer layer (Fig. S9E–F). The cross section of the outer layer is fairly homogenous.

The avian scutate scales are large and sub-rectangular (Fig. S10A). They show flaking on the outer surface (Fig. S10B–E). However, other than this flaking, the surface is not topographically complex and is very smooth, unlike the rippled texture of the outer surface of crocodile or even the avian reticulate scales. Even at high magnification, the only topographic variation appears to primarily come from flaking of the outer surface. The cross section shows a fairly well defined contact between the inner and outer layers (Fig. S10F). The outer layer appears to show splitting or flaking in cross section but is otherwise homogenous.

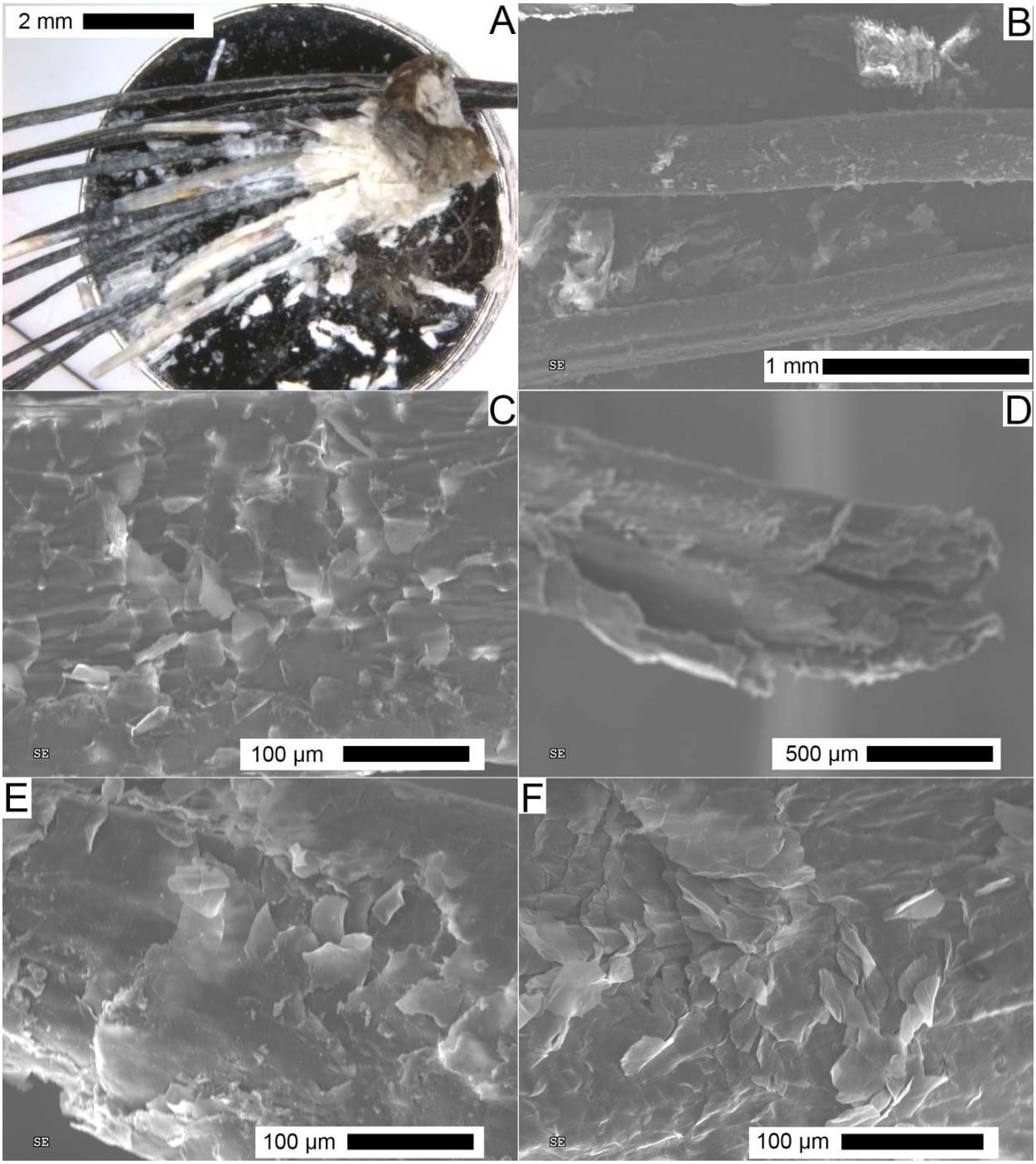

FIG. S1. Structural features of 'fresh' (although dried) adult turkey beard. A, under light microscopy, and B–F, SEM. B–C, bristle surfaces. D–E, bristle cross section. F, epidermal surface.

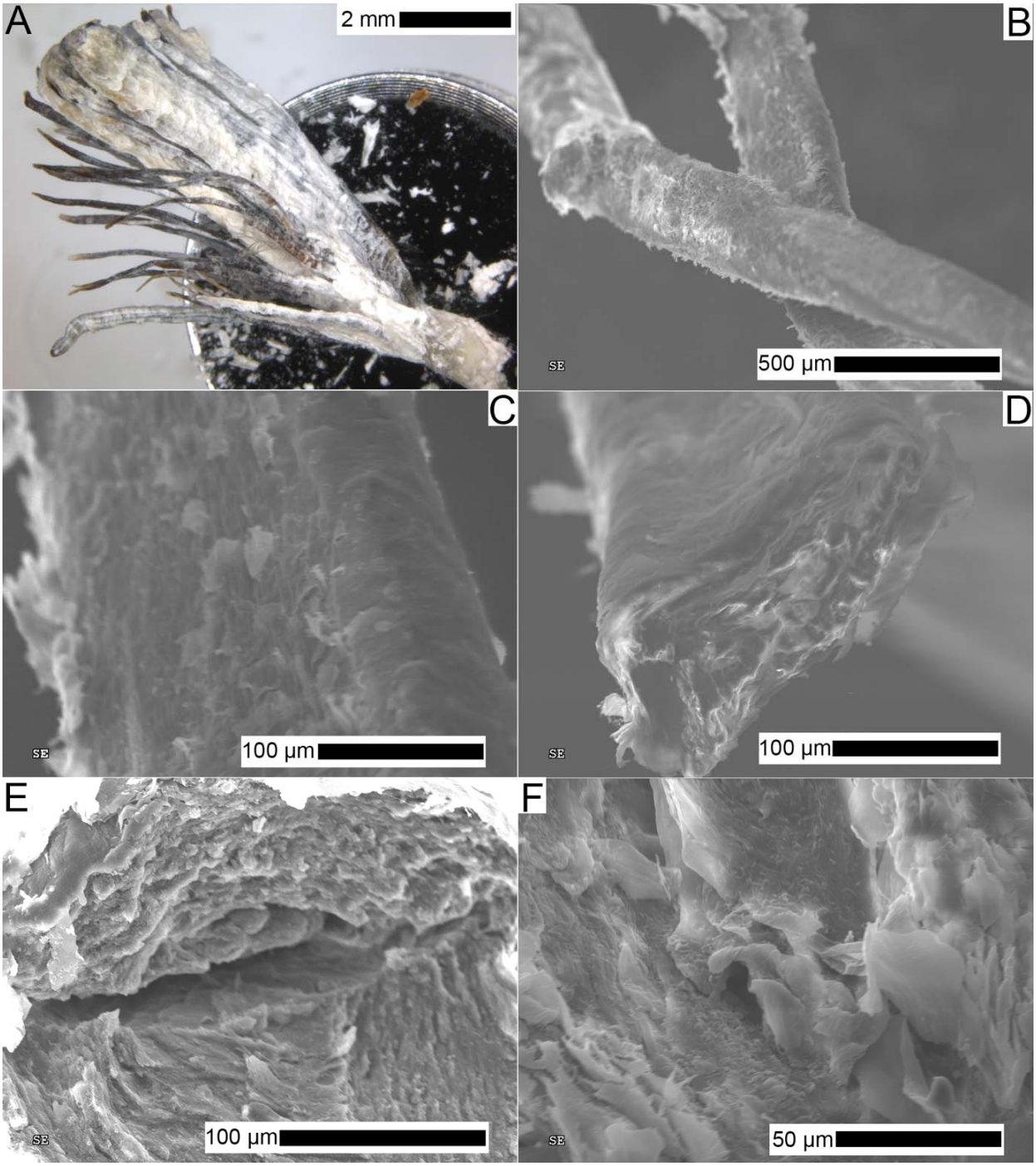

FIG. S2. Structural features of fresh juvenile turkey beard. A, under light microscopy, and B–F, SEM. B–C, bristle surfaces. D–E, bristle cross sections. F, epidermal surface.

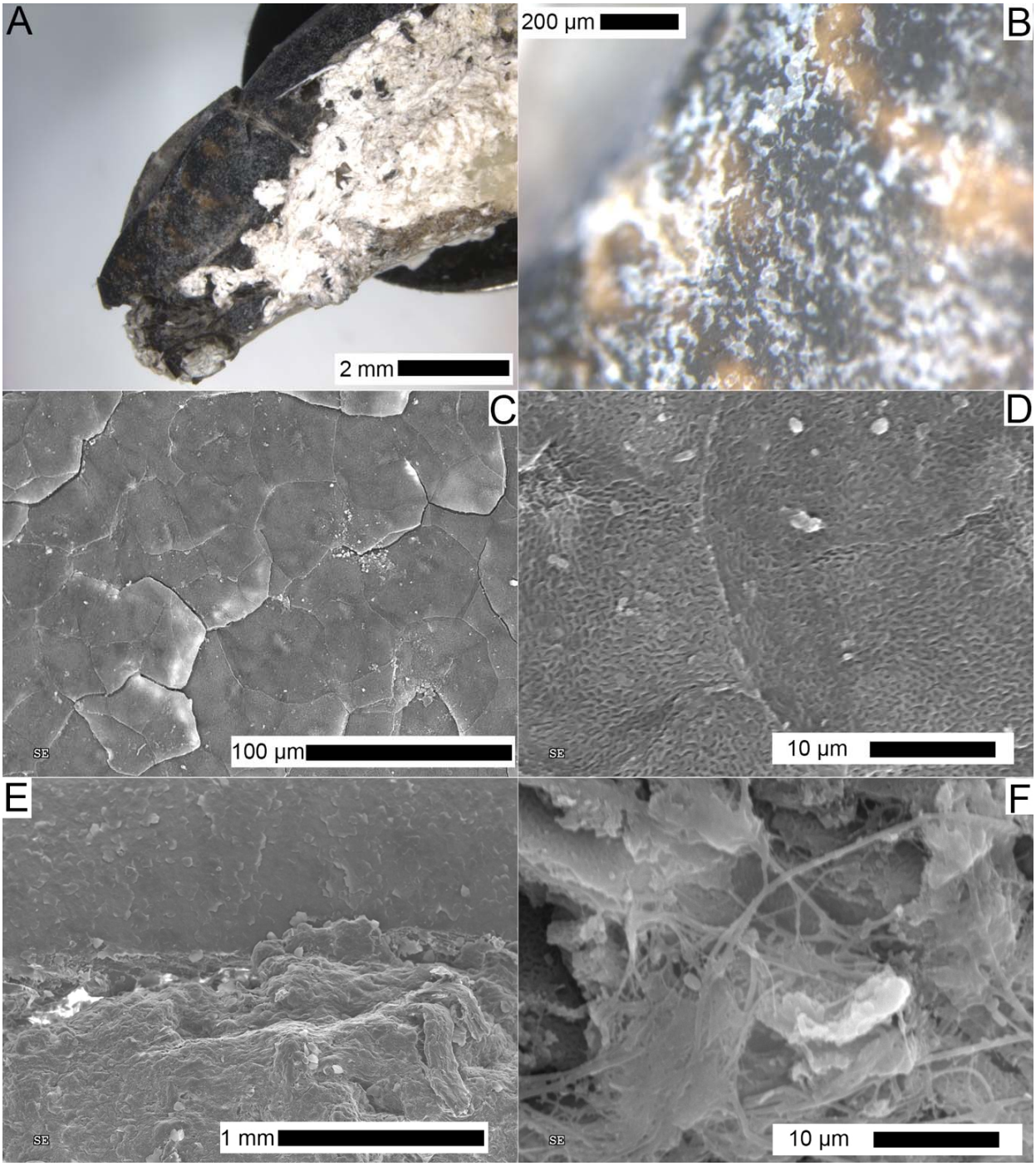

FIG. S3. Structural features of fresh predominantly black crocodile scale. A–B, under light microscopy, and C–F, SEM. A, cross section. B–D, outer surface. E, cross section at contact between outer (above) and inner (below) layers. F, cross section of inner layer.

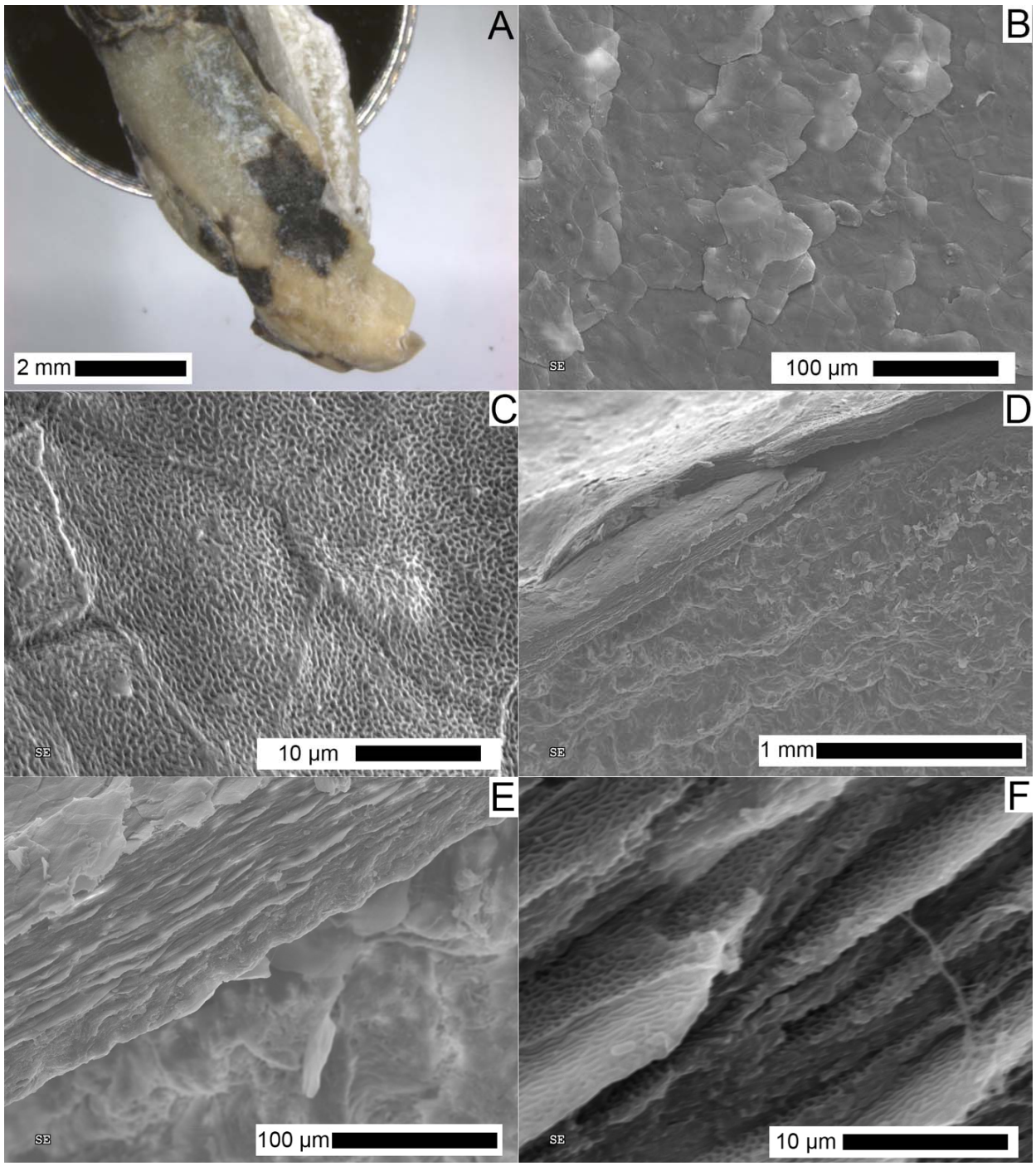

FIG. S4. Structural features of fresh predominantly white crocodile scale. A, under light microscopy, and B–F, SEM. A, view of outer surface in dorsal view with inner layer also visible to the right. B–C, outer surface. D–E, cross section at contact between outer (above) and inner (below) layers. F, cross section of outer layer.

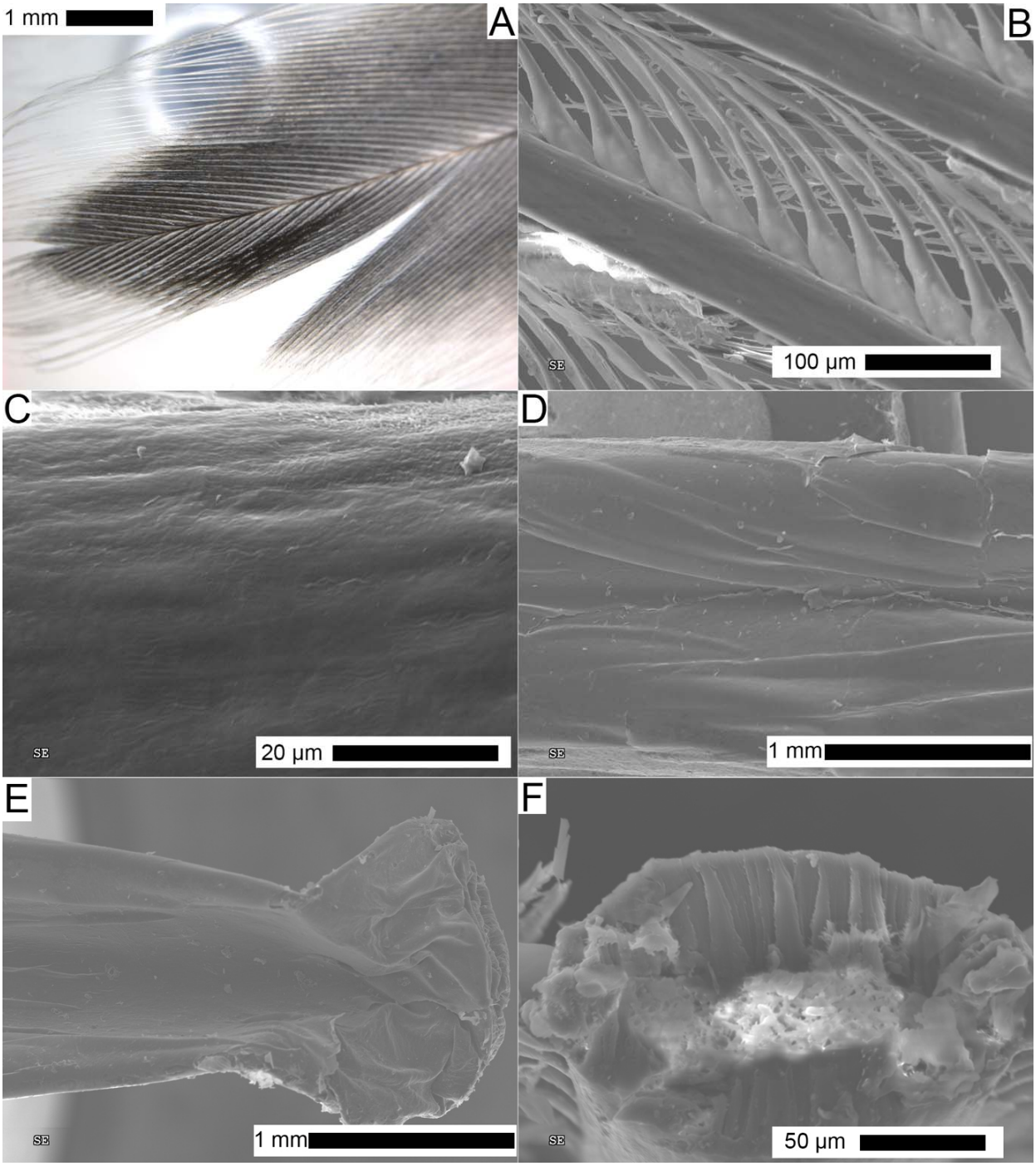

FIG. S5. Structural features of fresh black feather. A, under light microscopy, and B–F, SEM. A, white fringe to barbs is visible. B, pennaceous barbs and barbules. C, rachis surface at distal end. D–E, calamus surface. F, rachis cross section.

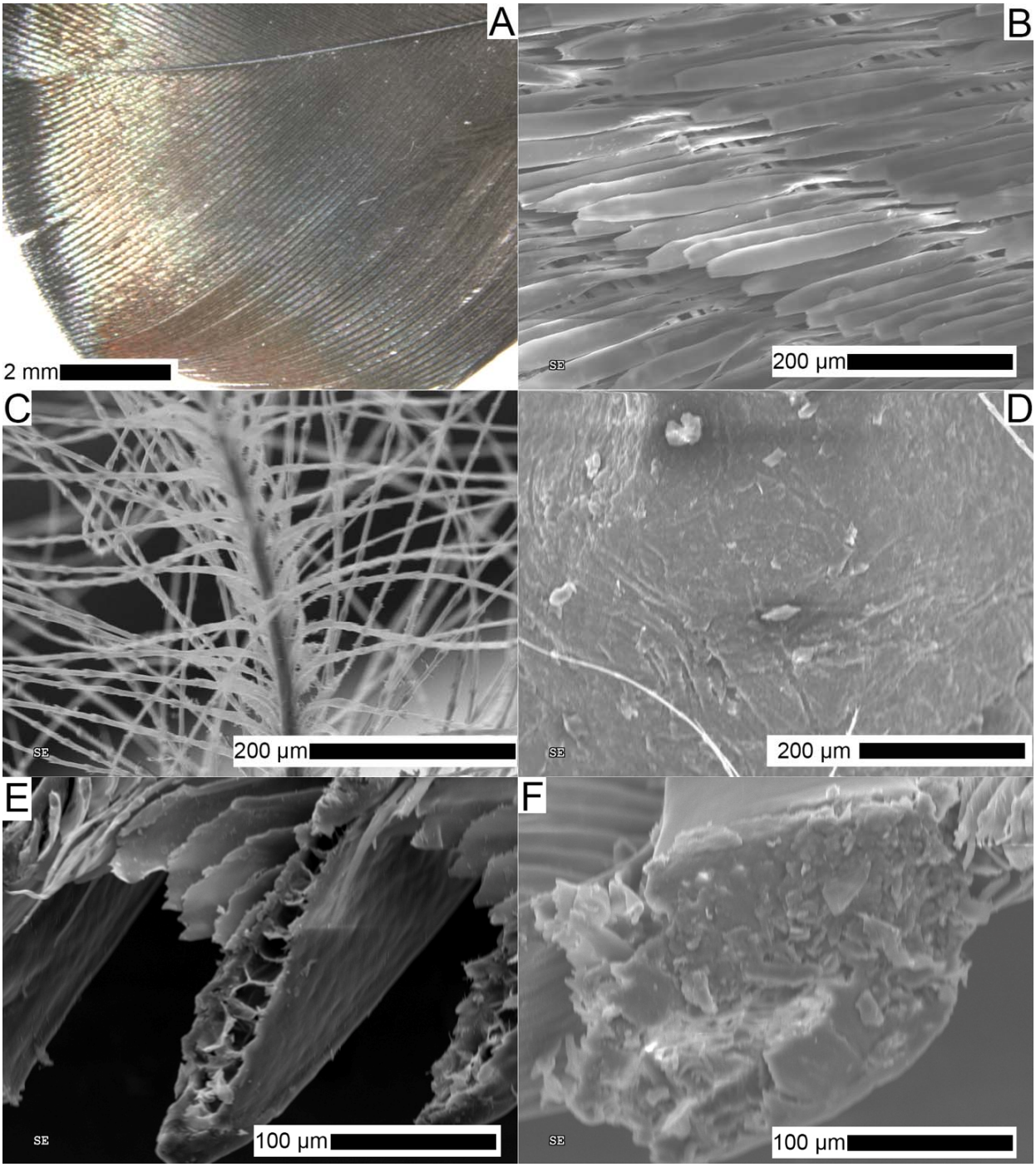

FIG. S6. Structural features of fresh iridescent feather. A, under light microscopy, and B–F, SEM. B, pennaceous barbules in iridescent region. C, plumulaceous barb and barbules. D, calamus surface. E, barb cross section. F, rachis cross section.

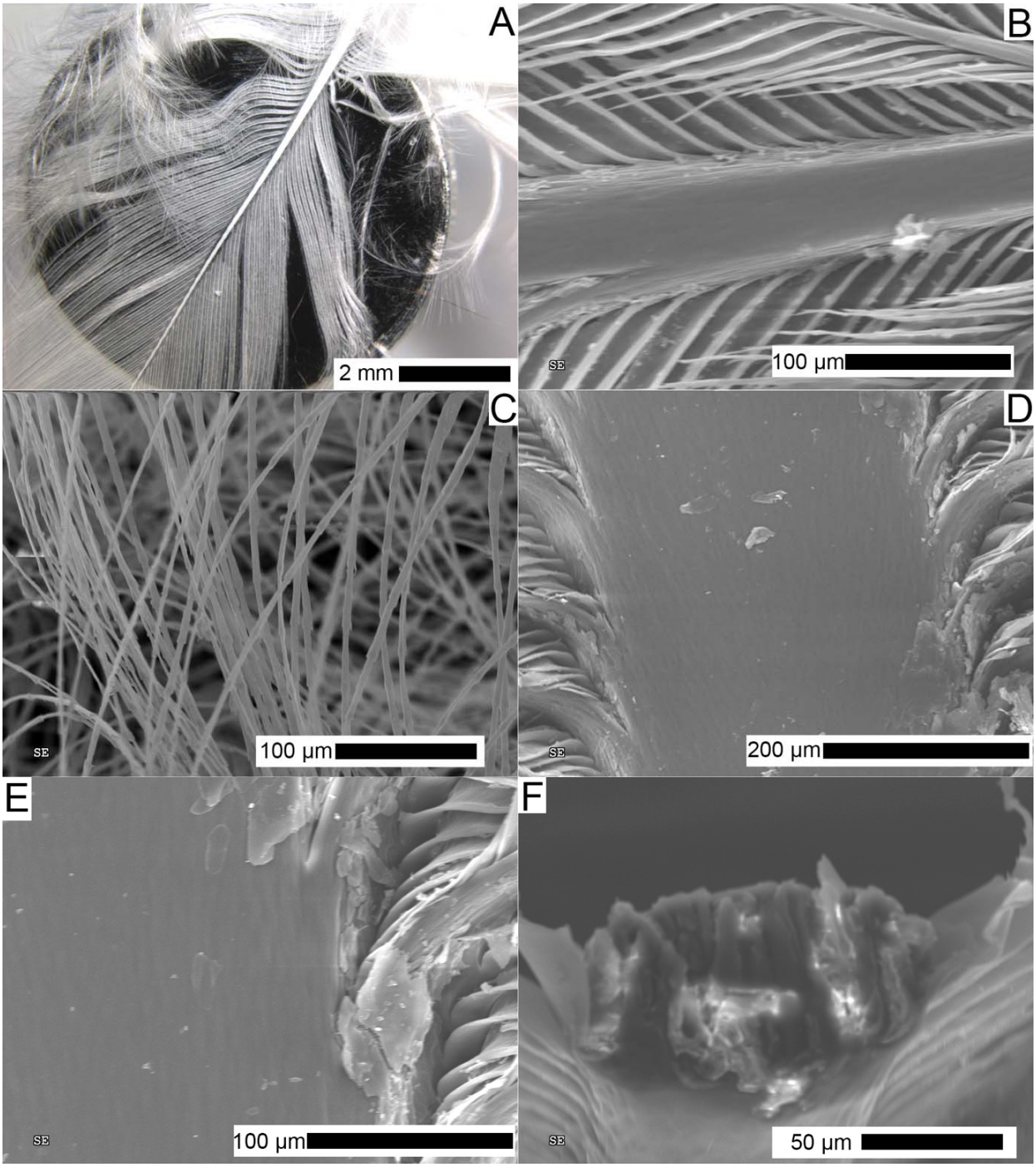

FIG. S7. Structural features of fresh white feather. A, under light microscopy, and B–F, SEM. B, rachis and pennaceous barbs and barbules. C, plumulaceous barbules. D–E, rachis surface. F, rachis cross section.

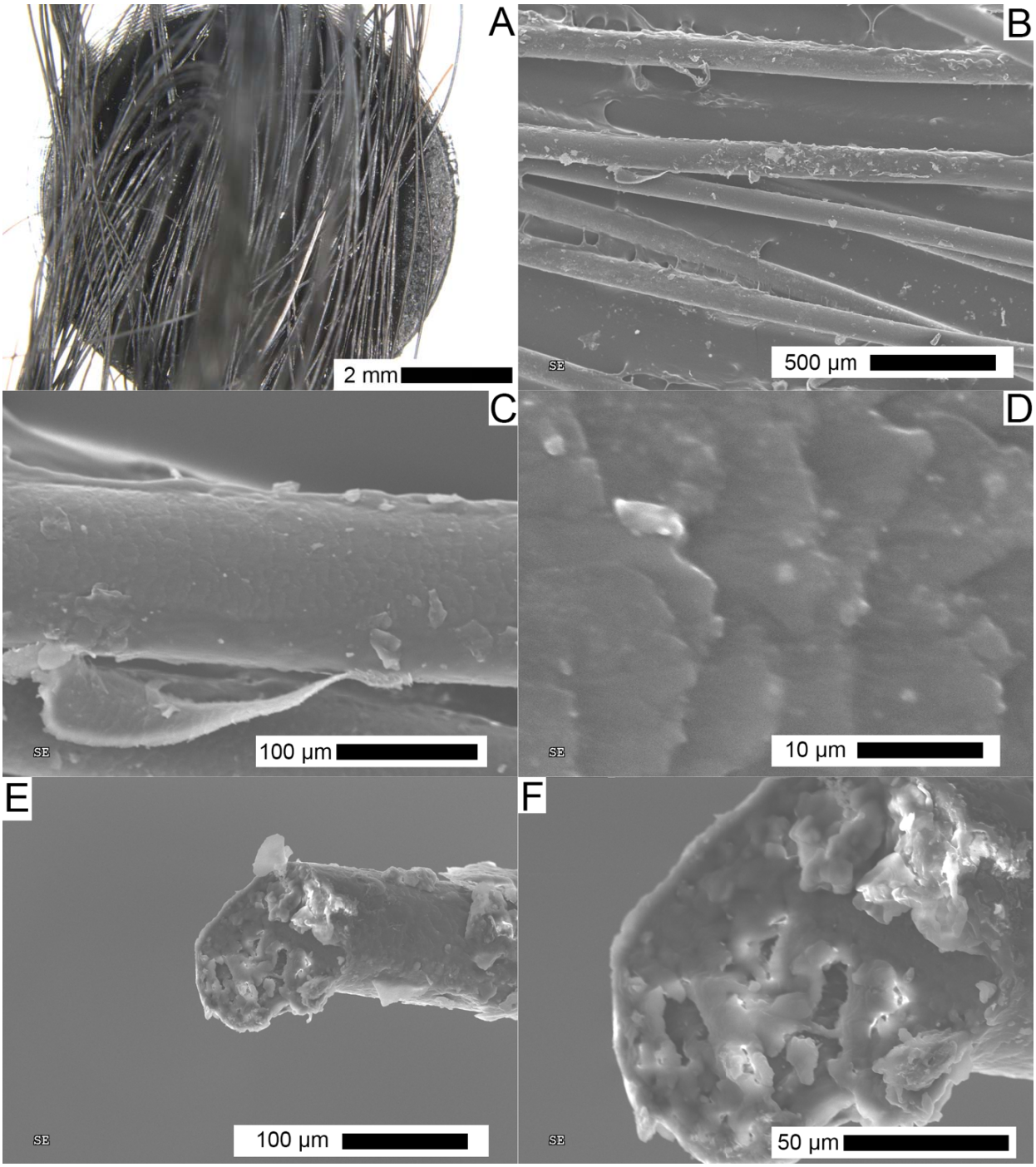

FIG. S8. Structural features of fresh horse hair. A, under light microscopy, and B–F, SEM. B–D, surface. E–F, cross section.

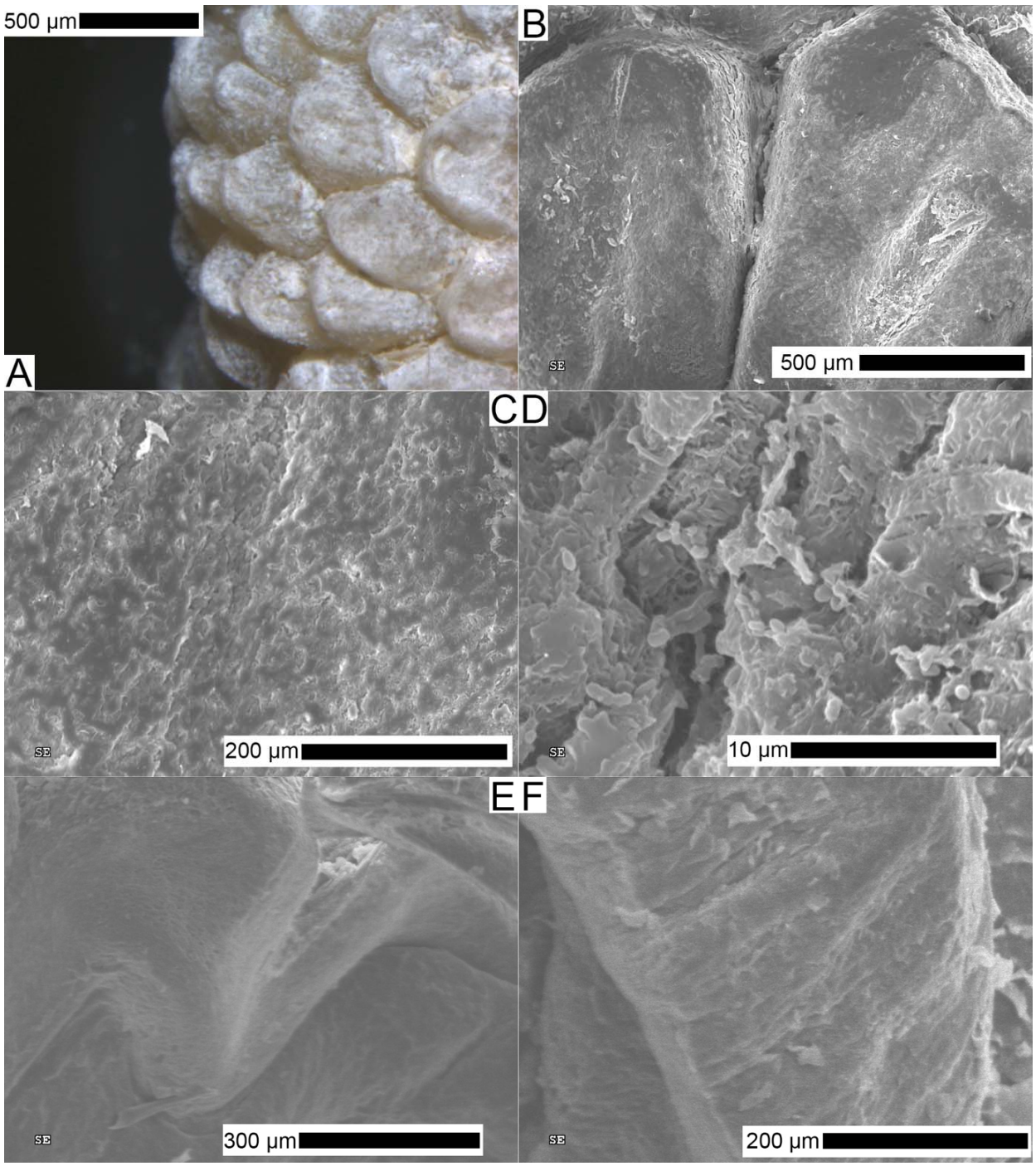

FIG. S9. Structural features of fresh avian reticulate scales. A, under light microscopy, and B–F, SEM. B–D, outer surface. E–F, cross section. E, exterior surface towards top of image. F, exterior surface towards right of image.

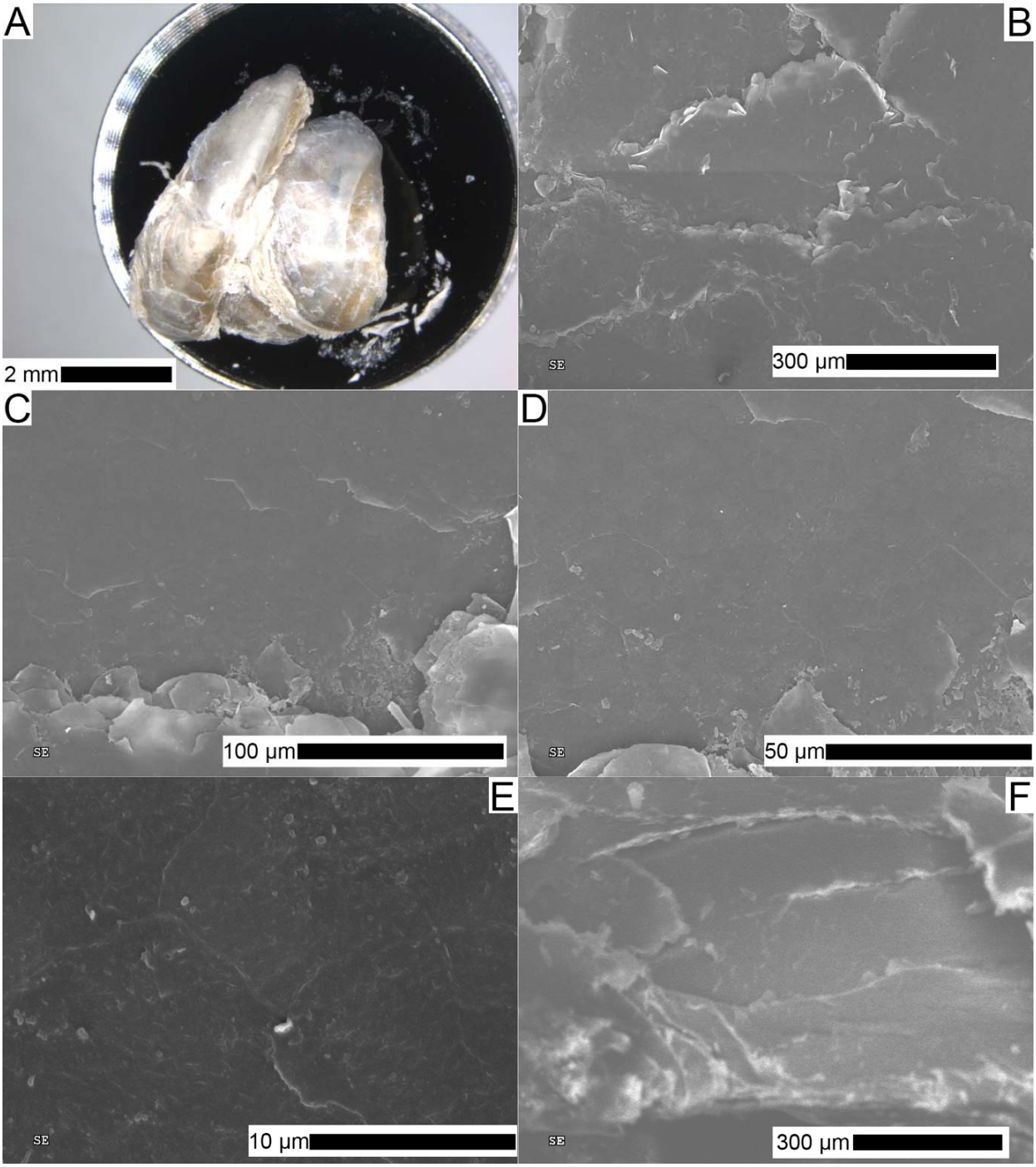

FIG. S10. Structural features of fresh avian scutate scales. A, under light microscopy, and B–F, SEM. B–E, outer surface. F, cross section with exterior surface towards top of image.

Decayed samples. The control feathers (darkly pigmented feathers in mineral water) showed no major signs of degradation even when examined in SEM. The feathers were still whole and showed full feather morphology (Fig. S38).

The decayed black feather showed the highest level of degradation, resulting in a lint-like mass of tiny feather bits (Fig. S11A). Most of this 'lint' was dark with only a few white remnants of the calamus or rachis present. When examining the sample only rinsed with ethanol after

decay, the dark bits appear to be barbs and barbules that are both interlocking as well as partially fused together (Fig. S11B). Upon higher magnification, the surface of the barbs appears to show extreme flaking (Fig. S11C–D), although the exact identity of some of these structures had to be further examined with the further prepared samples (see below). They could be bacteria, although this is unlikely given that bacteria would be expected to burst under the vacuum conditions of SEM. Bits of the rachis or calamus are apparent under SEM, and the surface shows a degraded, woven texture (Fig. S11E–F).

The sample of decayed black feather that was critically point dried after rinsing with ethanol appears to also show a flaking pattern to the keratin (Fig. S12A) distinct from well defined sausage-shaped structures that could either be melanosomes or bacteria (Fig. S12B–C). The structures can often be seen resting on a degraded keratin surface with a woven texture. The sample of decayed black feather that was rinsed with ethanol and then treated with Triton X-100 before critical point drying also shows these sausage-shaped structures (Fig. S12 D–F), proving that they are melanosomes and not bacteria. The degraded, woven texture of the keratin is also apparent in these samples.

The decayed iridescent feathers showed the second highest levels of degradation, resulting in small bits not quite as fine as the ‘lint’ produced from the decayed black feathers (Fig. S13A). The original feather structure was mostly lost, but more morphological structure was retained than in the decayed black feathers. As in the decayed black feathers, much of the remnants consisted of a mass barbs and barbules. Iridescence was even preserved (Fig. S13B). When examining the sample only rinsed with ethanol after decay, many pennaceous and plumulaceous barbules are apparent, such as the pennacous barbules consisting of the thickened ridge on one side that supports a flattened vane (Fig. S13C–D). Only a few remnants of the rachis are present and the surface appears relatively wrinkled (Fig. S13E–F).

The sample of decayed iridescent feather that was critically point dried after rinsing with ethanol shows fraying of the rachis surface (Fig. S14A), wrinkled keratin surface with potential bacteria or melanosomes on the surface (Fig. S14B), and exposed medulloid cells from the pith, some of which appear to be imploded (Fig. S14C). The sample of decayed iridescent feather that was rinsed with ethanol and then treated with Triton X-100 before critical point drying shows a degraded, woven texture to the keratin surface (Fig. S14D), plumulaceous barbules with well-preserved structure and some flaking on their surface (Fig. S14E), and many imploded medulloid cells exposed from the pith.

The decayed white feathers showed the lowest level of degradation among the experimental feathers. The entire macroscopic feather morphology was preserved (Fig. S15A), and the decayed white feathers were most similar to the control feathers in the mineral water in terms of level of degradation. Examining the sample only rinsed with ethanol after decay revealed that the calamus surface appears to be flaking (Fig. S15B–C). However, much of the keratin surface appears to be relatively unaltered (Fig. S15D). Interestingly, one region of the rachis surface shows short, hair-like structures extending off of the surface when viewed under high magnification (Fig. S15E). The cross section of the rachis is typical with an outer cortex showing a columnar, radiating structure and and inner pith filled with medulloid cells (Fig. S15F).

The sample of decayed white feather that was critically point dried after rinsing with ethanol shows similar features to the sample simply rinsed in ethanol and reveals little keratin surface degradation on the barbs, barbules, and rachis (Fig. S16A–C). It also shows a normal rachis cross section with outer cortex and pith represented (Fig. S16D). The sample of decayed

white feather that was rinsed with ethanol and then treated with Triton X-100 before critical point drying provides similar information. The calamus surface shows little degradation (Fig. S16E–F).

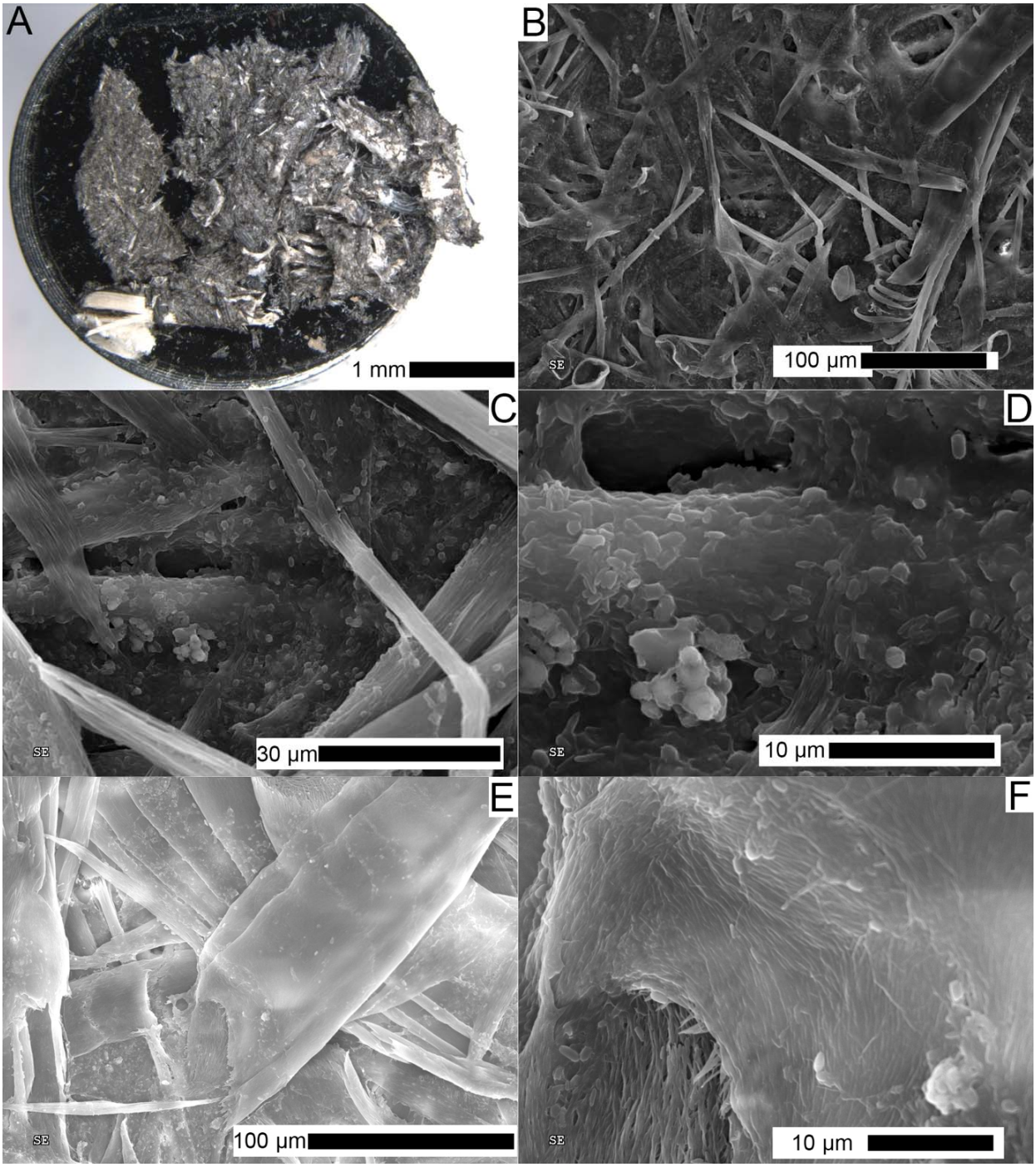

FIG. S11. Structural features of decayed black feathers rinsed with ethanol after decay treatment. A, under light microscopy, and B–F, SEM. B–D, fused mass of barbules. E–F, rachis or calamus surface.

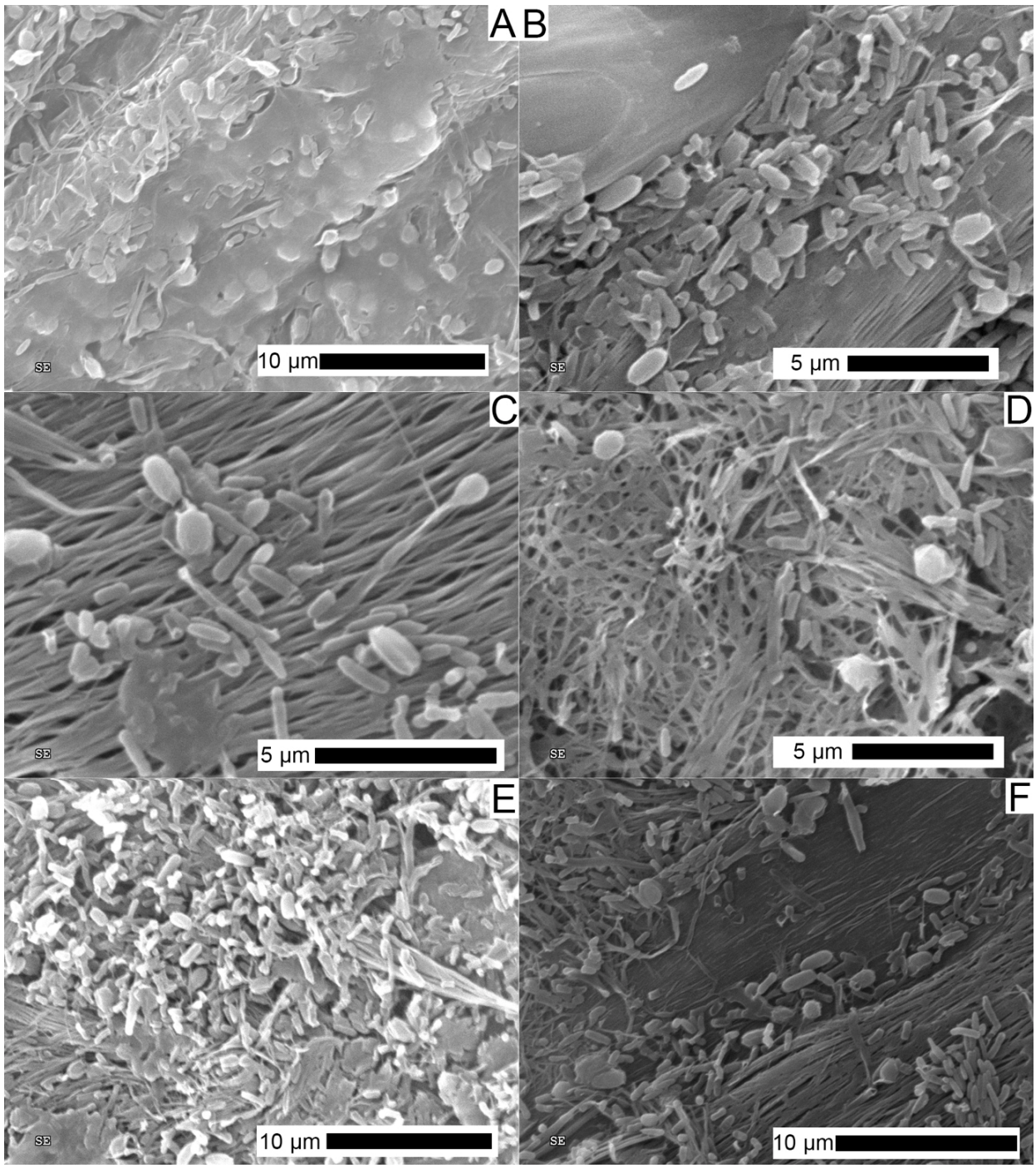

FIG. S12. SEM images of structural features of decayed black feathers rinsed with ethanol after decay treatment and then prepared further. A–C, samples critically point dried. D–F, samples treated with Triton X-100 detergent and then critically point dried.

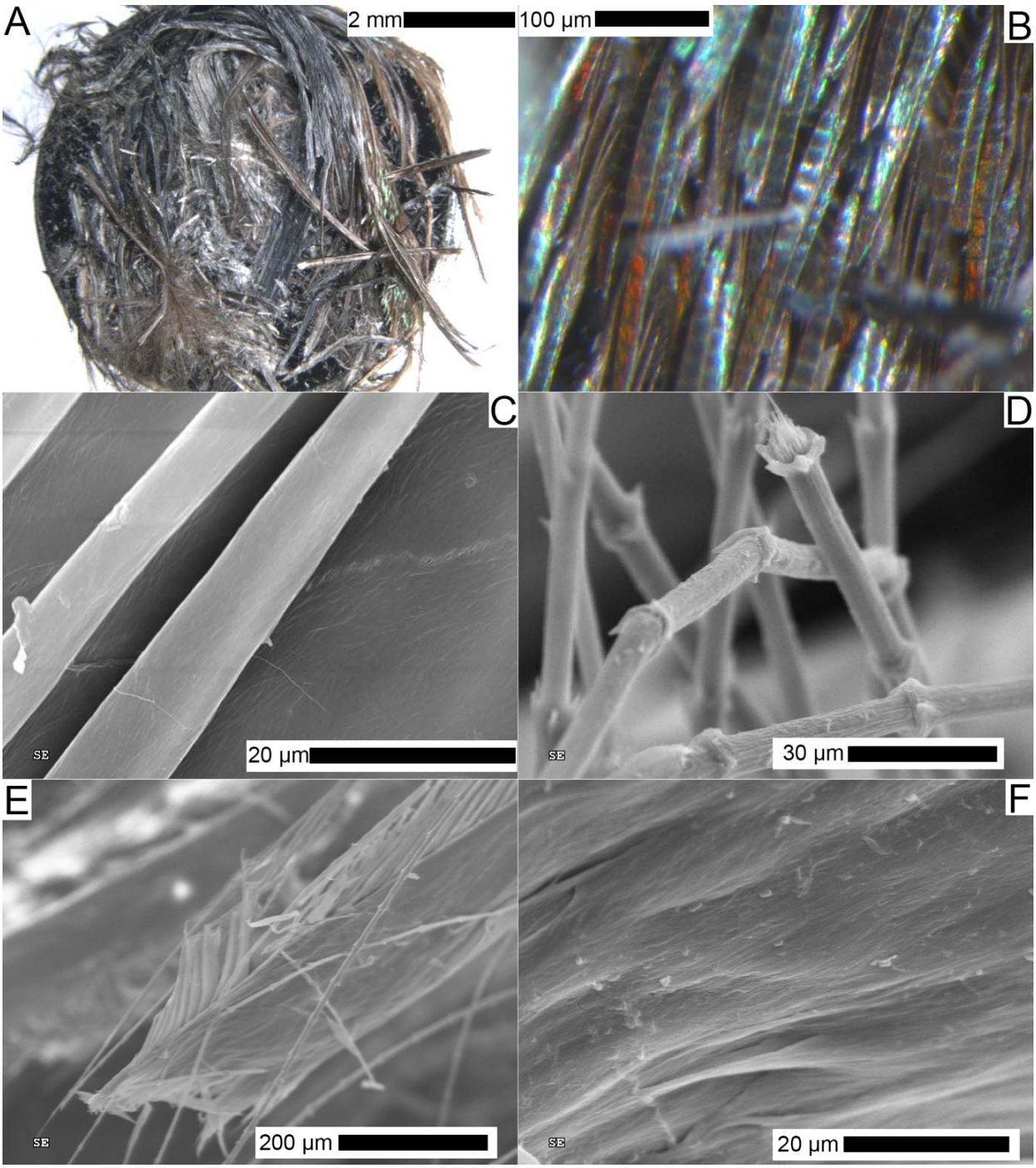

FIG. S13. Structural features of decayed iridescent feathers rinsed with ethanol after decay treatment. A–B, under light microscopy, and C–F, SEM. B, iridescent pennaceous barbules. C, pennaceous barbules. D, plumulaceous barbules. E–F, rachis surface.

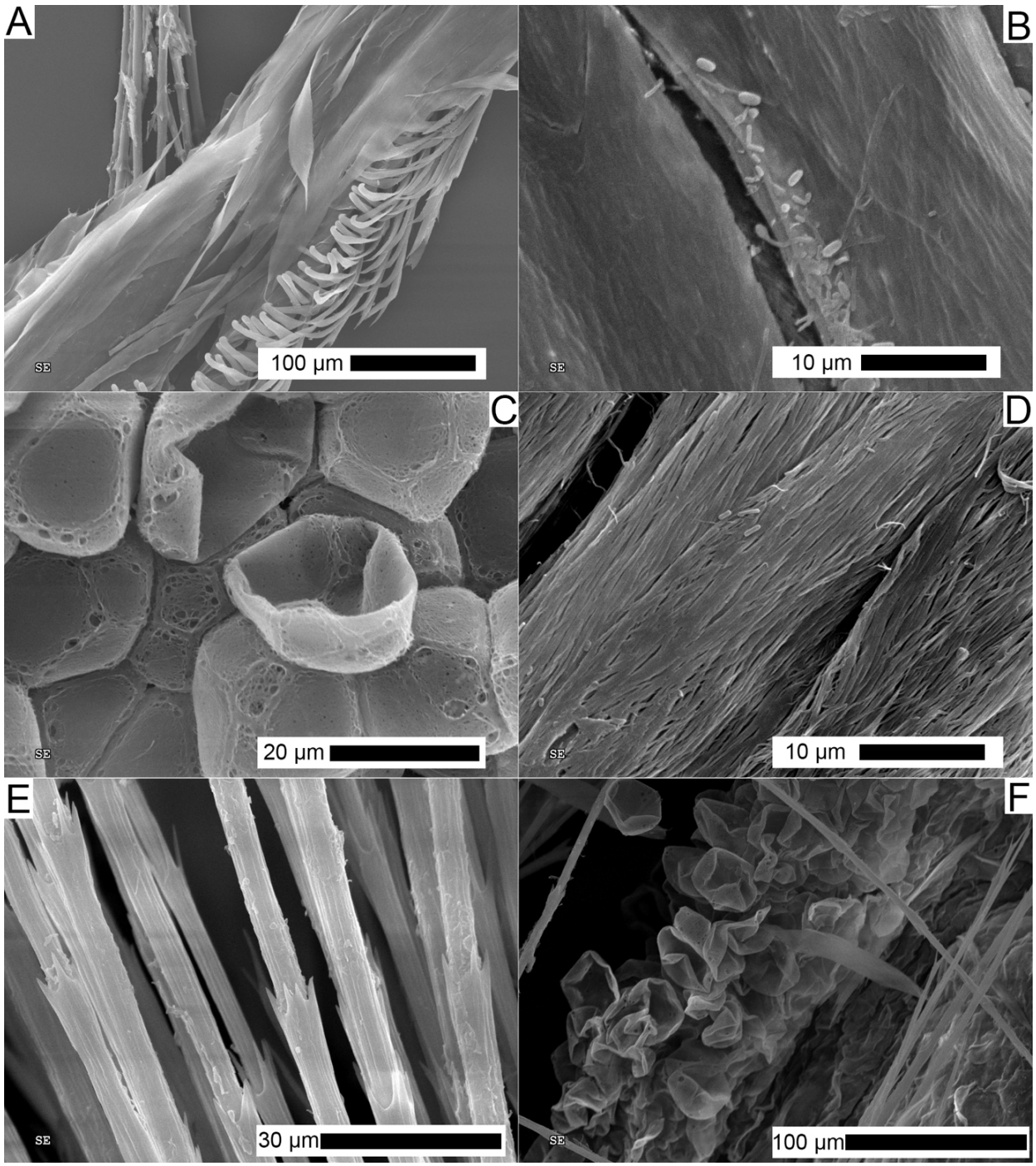

FIG. S14. SEM images of structural features of decayed iridescent feathers rinsed with ethanol after decay treatment and then prepared further. A–C, samples critically point dried. D–F, samples treated with Triton X-100 detergent and then critically point dried.

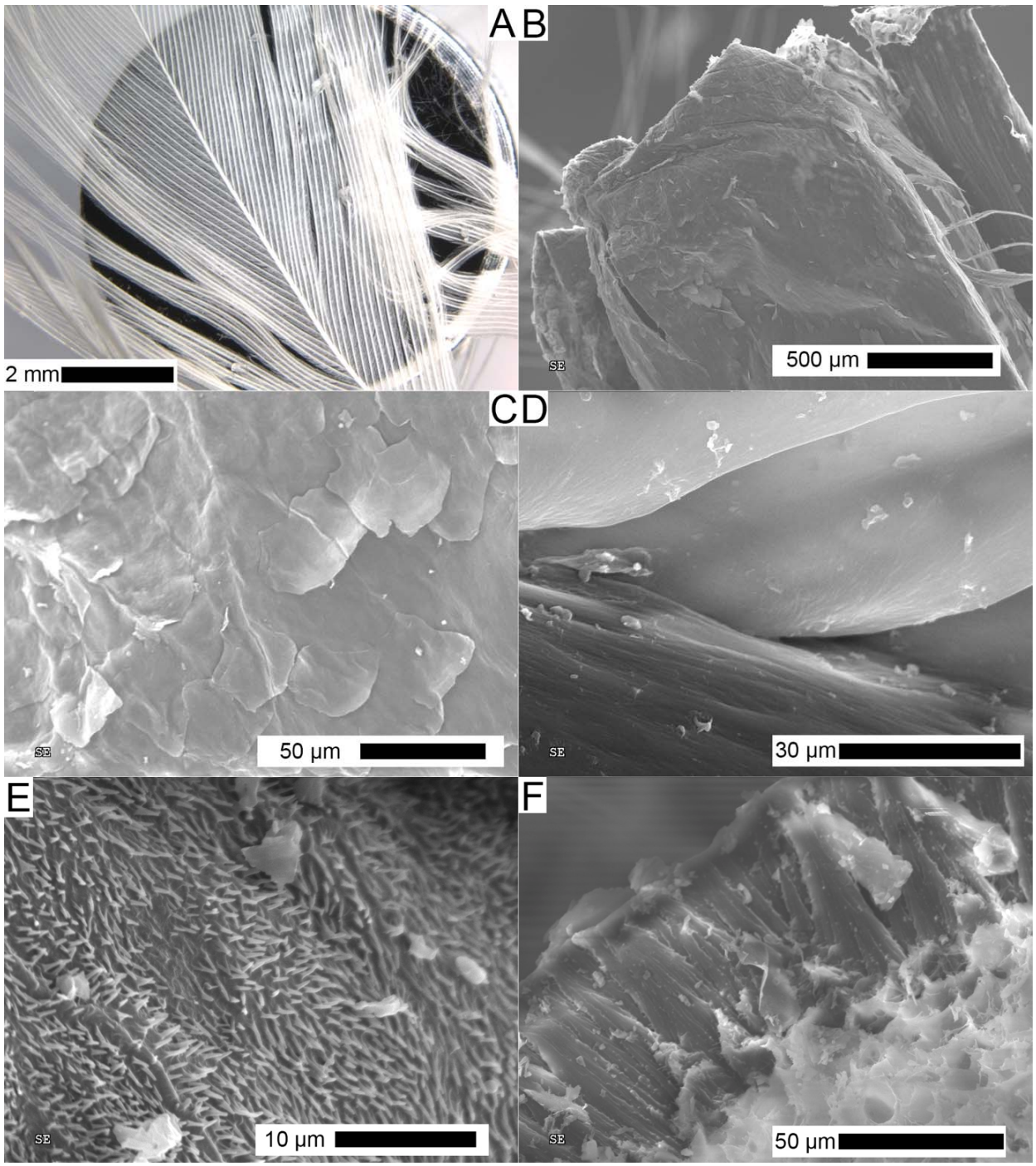

FIG. S15. Structural features of decayed white feathers rinsed with ethanol after decay treatment. A, under light microscopy, and B–F, SEM. B–C, calamus surface. D, pennaceous barb and barbules. E, rachis surface. F, rachis cross section.

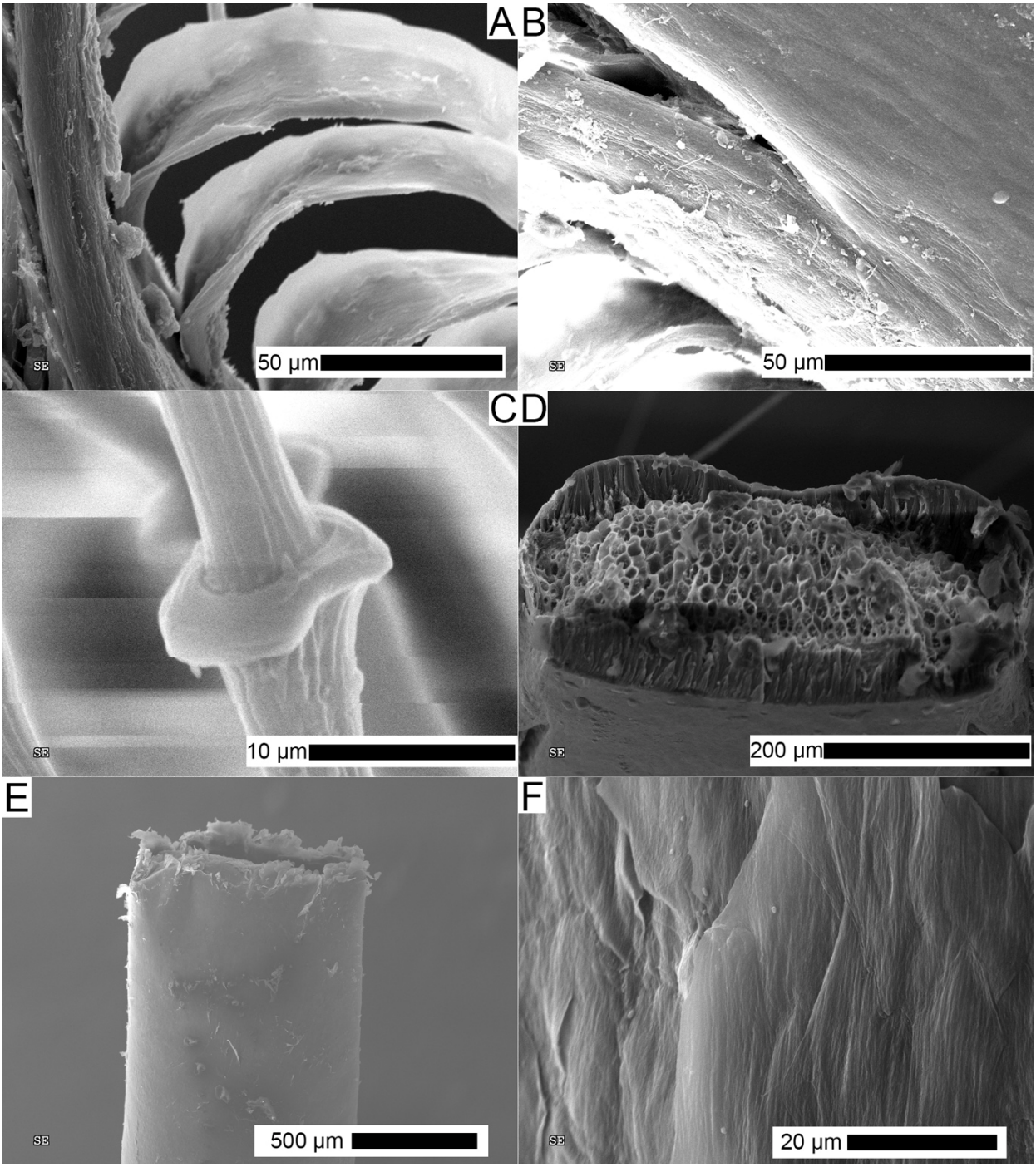

FIG. S16. SEM images of structural features of decayed white feathers rinsed with ethanol after decay treatment and then prepared further. A–D, samples critically point dried. E–F, samples treated with Triton X-100 detergent and then critically point dried. A, pennaceous barb and barbules. B, rachis and barb surface. C, plumulaceous barbule. D, rachis cross section. E–F, calamus surface.

Matured samples. The following are maturation experiments at 100°C/250 bars for 24 hours (i.e., moderately matured).

The moderately matured adult turkey beard showed bristles with a wrinkled texture (Fig. S17A). In addition to wrinkling, the bristles appear to be flaking (although some of this might be matured epidermis adhering to the bristles) (Fig. S17B–C). The bristle cross section is strongly compressed in some areas (Fig. S17D), and this particular example shows how some bristles are not completely solid, but can have a hollow central region. The epidermis is extremely degraded and consists of thin flakes (Fig. S17E–F).

The moderately matured juvenile turkey beard shows curling in the bristles and discolored epidermis (Fig. S18A). The tight curls of the bristles are accompanied by degradation of the bristle surface as seen by the rough texture (Fig. S18B–C). The cross sections of the bristles are solid and compressed, but the keratin still appears somewhat organized (Fig. S18D–E). The epidermis is degraded and appears to be flaking similar to that seen in the matured adult turkey beard (Fig. S18F).

The moderately matured predominantly black crocodile scale retains some of it's original color variation (Fig. S19A). The hard outer layer shows splitting between its sub-layers and cracking (Fig. S19B–C). The rippled texture of the outer layer's surface was still retained in some areas (Fig. S19D). The internal layer of the scale can be distinguished from the hard outer layer and shows a lot of degradation (Fig. S19E). This internal layer has become soft (Fig. S19F).

The moderately matured predominantly white crocodile scale consists of harder and softer products representing the outer and inner layers of the scale, respectively, and retains its light coloration on it's outer layer, although some discoloration appears to have occurred (Fig. S20A–B). The outer layer shows cracking, flaking, and splitting between its sub-layers (Fig. S20C). These sub-layers still retain the original rippled texture (Fig. S20D). The inner layer is more degraded and exhibits pock-marking (Fig. S20E–F).

The moderately matured black feather shows a breakdown of the overall feather structure, retention of original coloration variation, and curling of the keratin (Fig. S21A). Many subunits of the feather are still present, however, such as barbs and barbules, although these are incomplete and show curling and kinking (Fig. S21B–F). The rachis could not be found in the sample.

The moderately matured decayed black feather shows extreme degradation resulting in a black pellet (Fig. S22A). Some of it consists of a mass of fused barbs and barbules (Fig. S22B), although other areas appear to derive from the rachis and have a flat surface with cracks (Fig. S22C). Yet other regions show a granulated texture (Fig. S22D). Only a small amount of original structure remains, such as some barbules attached to barbs, but these have highly degraded surfaces and are flattened (Fig. S22E–F).

The moderately matured iridescent feather consists of clumped, folded barbs and some of the iridescence remains (Fig. S23A). The morphology of the barbs at low magnification appears relatively well conserved, despite maturation. The barbs are closely packed together and the barbs and barbules are often incomplete (Fig. S23B–D). One portion of the sample appears to represent part of the rachis (Fig. S23E). The keratin shows signs of degradation such as wrinkling on the barbs and barbules surfaces (Fig. S23D) and flaking of the rachis (Fig. S23F).

The moderately matured decayed iridescent feather may have been exposed to water during autoclaving as the capsule gained weight, suggesting a failed seal and infiltration of water (Table S1). However, the sample was analyzed anyway. The sample shows extreme degradation resulting in a black pellet (Fig. S24A) similar to that seen in the moderately matured decayed black feather. The keratin surface of what appears to be the remnants of the rachis is cracked and

fraying into strips or strands (Fig. S24B–C) These strands are irregular in cross-sectional shape with folding and creases common and are sometimes associated with thin filaments (Fig. S24D–E). Some degraded barbules attached to remnants of barbs are visible and the barbules appear shriveled (Fig. S24F).

The moderately matured white feather shows high levels of degradation and the predominant remnant is the rachis/calamus (Fig. S25A). However, some plumulaceous barbs are still apparent whose surfaces are moderately degraded as evidenced by minor wrinkling and flaking (Fig. S25B–C). The surface of the calamus is highly degraded with wrinkling, cracking, flaking, and fraying apparent (Fig. S25D–F). The fraying produces strips of keratin like those seen in the moderately matured decayed iridescent feather.

The moderately matured decayed white feather appears similar to the matured white feather at low magnification with predominantly the rachis/calamus surviving (Fig. S26A). However, it appears to show the highest levels of degradation at the ultrastructural level of all the feather samples examined in this study other than the highly matured ‘goo’ derived from feathers. Plumulaceous barbs are still apparent at one end of the sample (Fig. S26B). However, the surface of the calamus shows a woven, and in some places cracked, texture and the proximal end shows internal layering of strands (Fig. S26C–F) that at first seem similar to the strands seen in the moderately matured white feather and the moderately matured decayed iridescent feather. However, these strands appear to be well organized and overlapping with regularly spaced nodes. Overall they appear almost identical to plumulaceous barbules (Fig. S26E). These strands can be observed originating from more continuous and less degraded regions of the calamus (Fig. S26D).

The moderately matured horse hair shows curling and extreme kinking in the strands (Fig. S27A–B). Some strands are split down their length (Fig. S27C) and the keratin surface is flaked (Fig. S27D). The kinks sometimes occur in a helical pattern down the strand (Fig. S27E). The cross section of the strand is solid, yet disorganized (Fig. S27F).

The moderately matured avian reticulate scales are highly degraded and show softer and harder remnants under high magnification, representing the inner and outer layers of the scales, respectively (Fig. S28A). However, overall the sample is much more pliable than the fresh avian reticulate scales. The harder remnants show flaking at the surface and the original sub-layering is revealed with wrinkled surface texture (Fig. S28B–C). The softer remnants are clumped (Fig. S28D) and show many pock-marks on their surface (Fig. S28E). In addition to pock-marks, bulges and folds of the organic material are also apparent along with structures intermediate between the pock-marks and the bulges (Fig. S28F).

The moderately matured avian scutate scale is also highly degraded and shows a more pliable structure than the fresh avian scutate scales (Fig. S29A) with potentially harder and softer remnants observable under high magnification deriving from the outer and inner layers, respectively. The surface is wrinkled and flaking and some areas show a rough texture, representing degradation (Fig. S29B–F).

Regarding the highly matured samples (250°C/250 bars for 24 hours), neither the ‘goo’ derived from the dark nor the white feathers show microscopic features such as exposed melanosomes, and the only topography derives from uneven dispersal of the ‘goo’ across the capsule surface (Fig. S30A–F). A sample of white feathers matured at 200°C/250 bars for 24 hours also produced a ‘goo’ that unfortunately leaked from the autoclave tube and could not be analyzed.

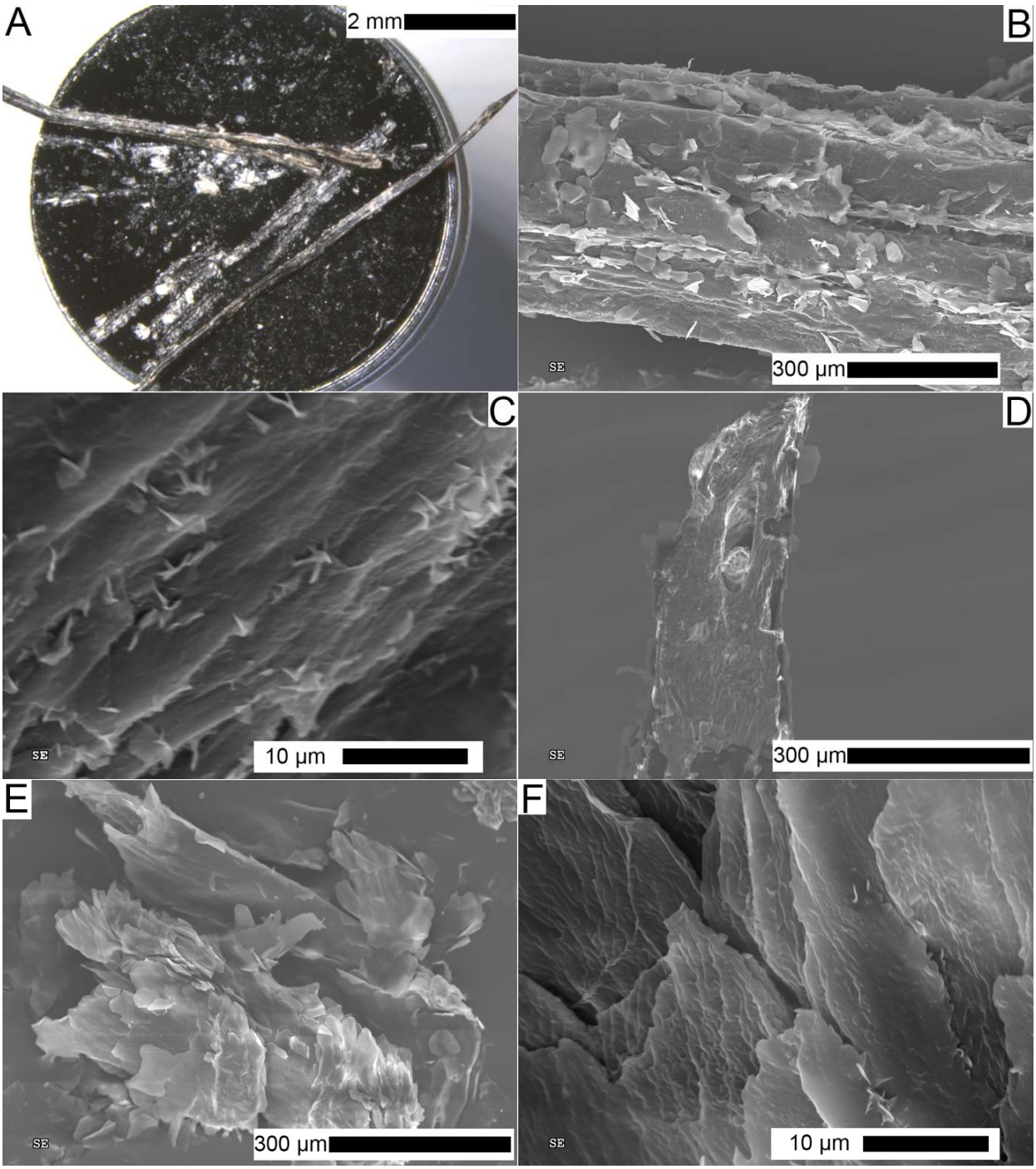

FIG. S17. Structural features of moderately matured adult turkey beard. A, under light microscopy, and B–F, SEM. B–C, bristle surfaces. D, bristle cross section. E–F, epidermal surface.

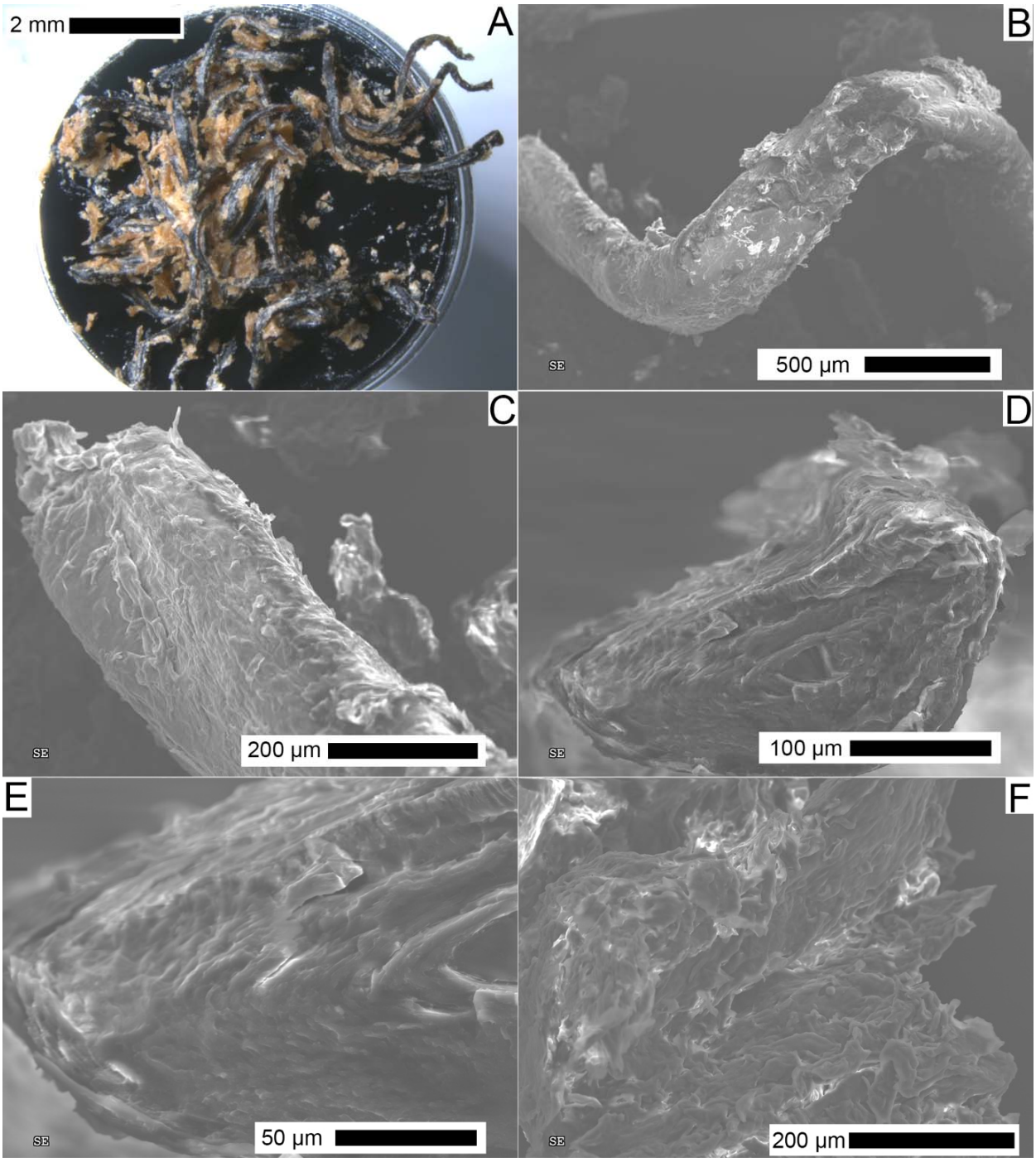

FIG. S18. Structural features of moderately matured juvenile turkey beard. A, under light microscopy, and B–F, SEM. B–C, bristle surfaces. D–E, bristle cross section. F, epidermal surface.

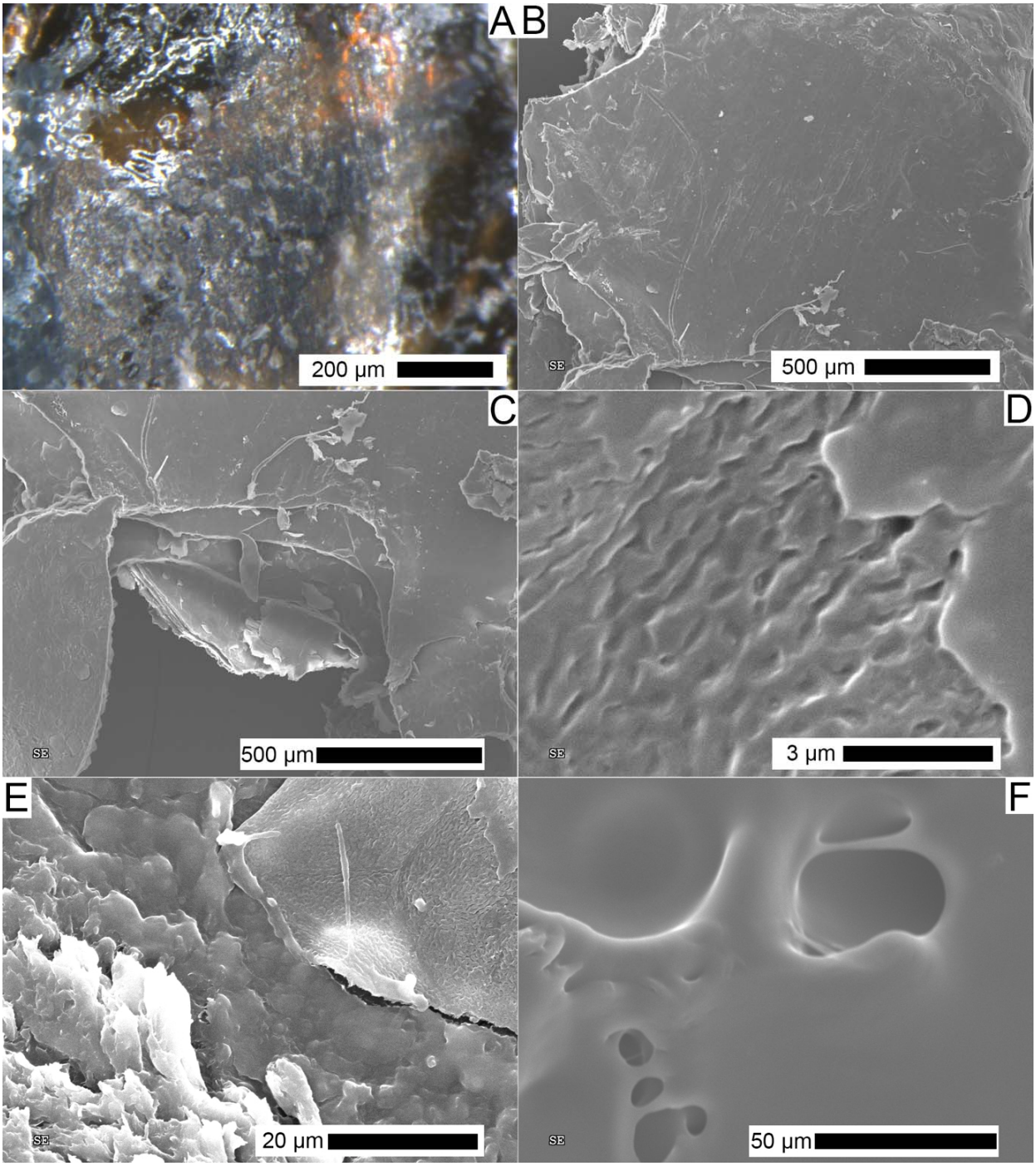

FIG. S19. Structural features of moderately matured predominantly black crocodile scale. A, under light microscopy, and B–F, SEM. A–D, harder remnants. E, softer and harder remnants. F, softer remnants.

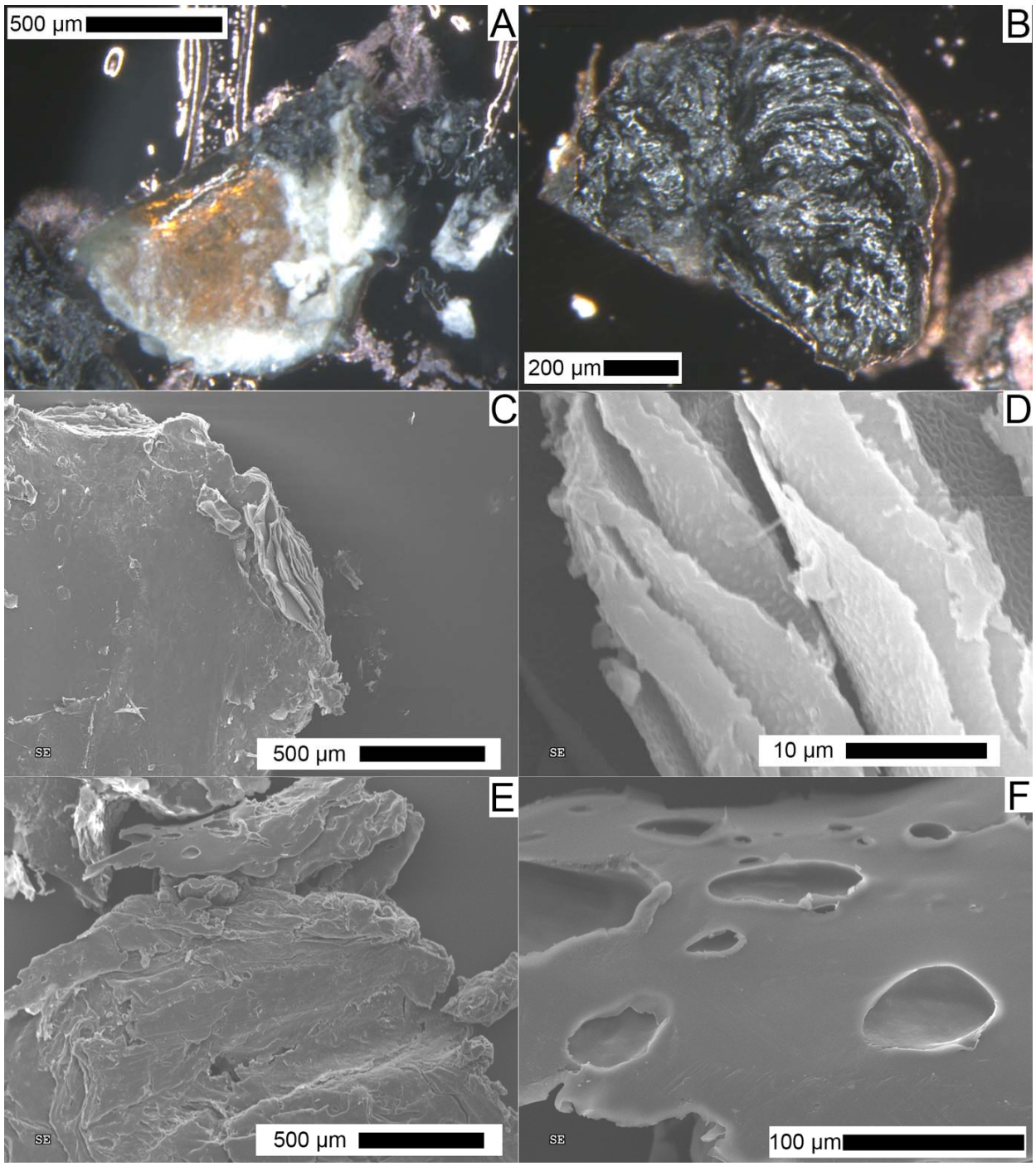

FIG. S20. Structural features of moderately matured predominantly white crocodile scale. A, under light microscopy, and B–F, SEM. A, C–D, harder remnants. B, E–F, softer remnants.

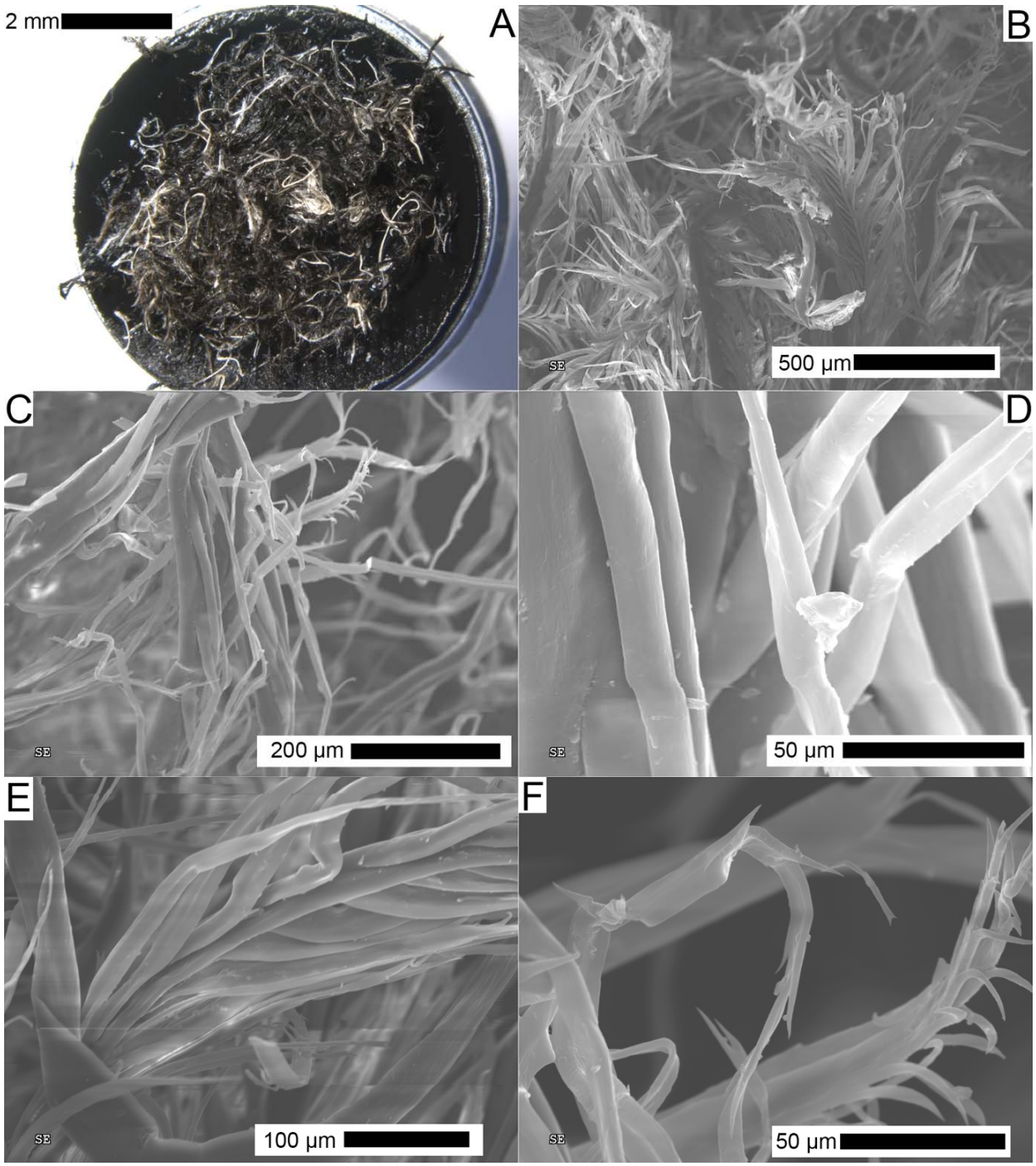

FIG. S21. Structural features of moderately matured black feather. A, under light microscopy, and B–F, SEM.

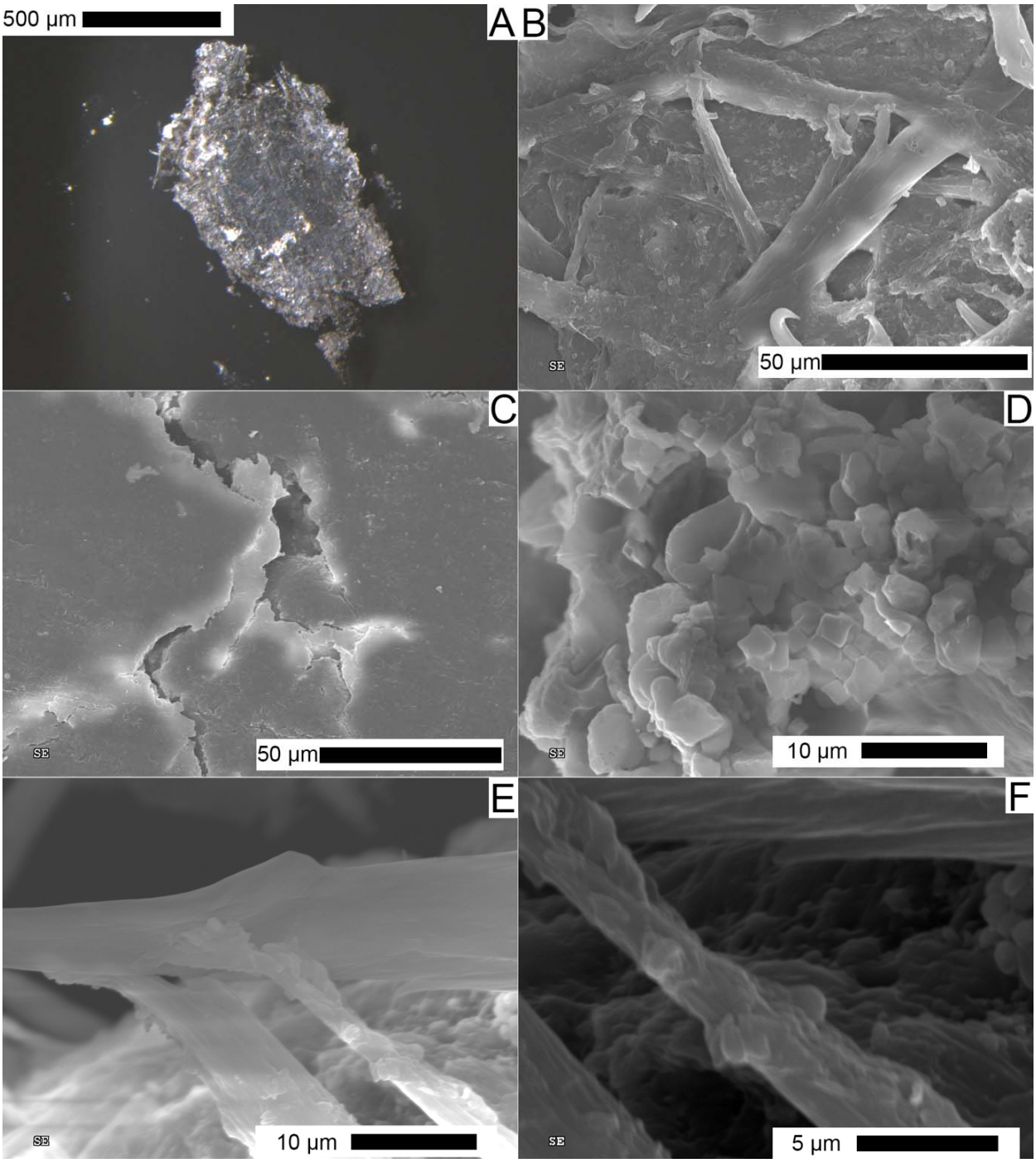

FIG. S22. Structural features of moderately matured decayed black feather. A, under light microscopy, and B–F, SEM.

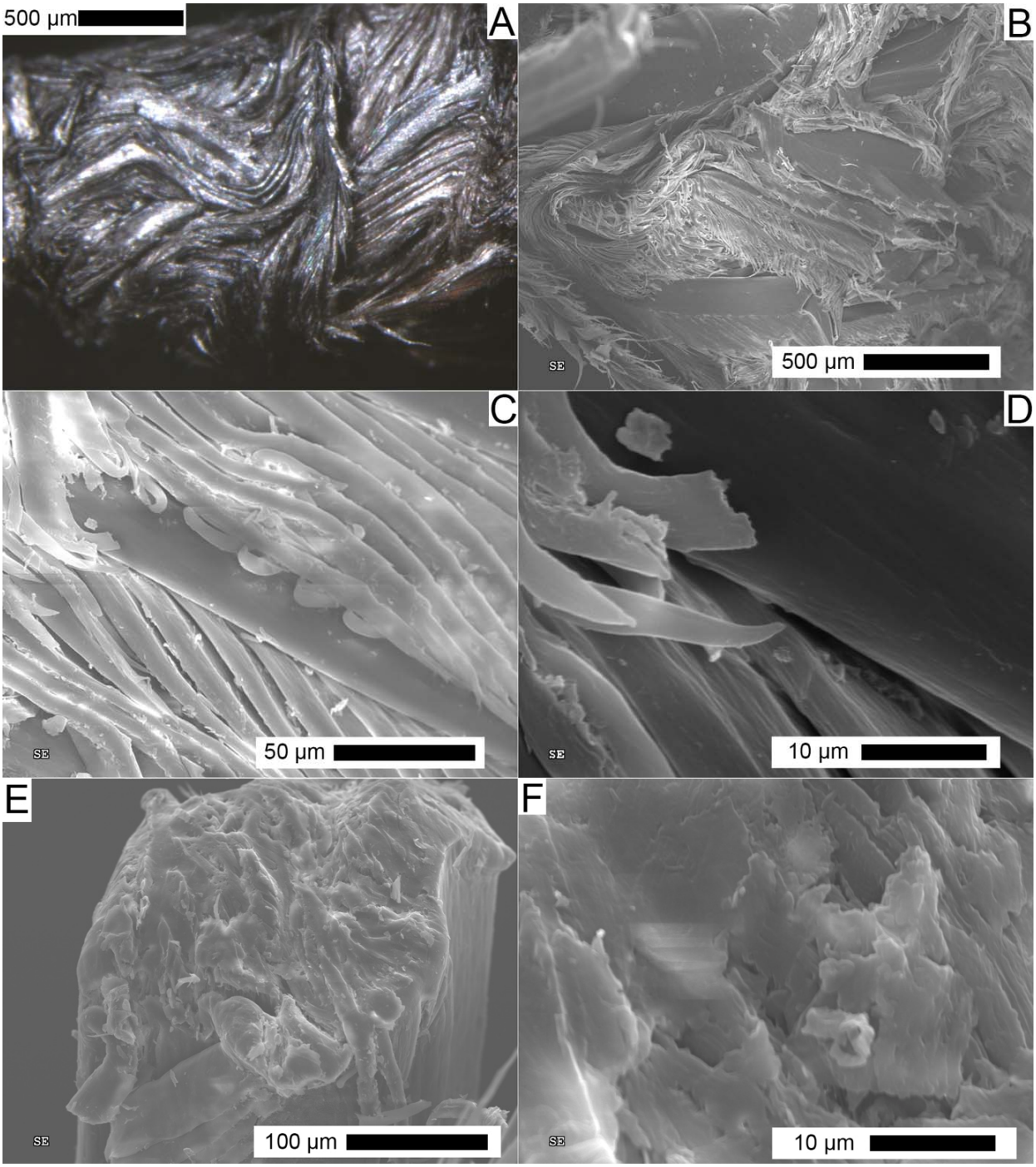

FIG. S23. Structural features of moderately matured iridescent feather. A, under light microscopy, and B–F, SEM.

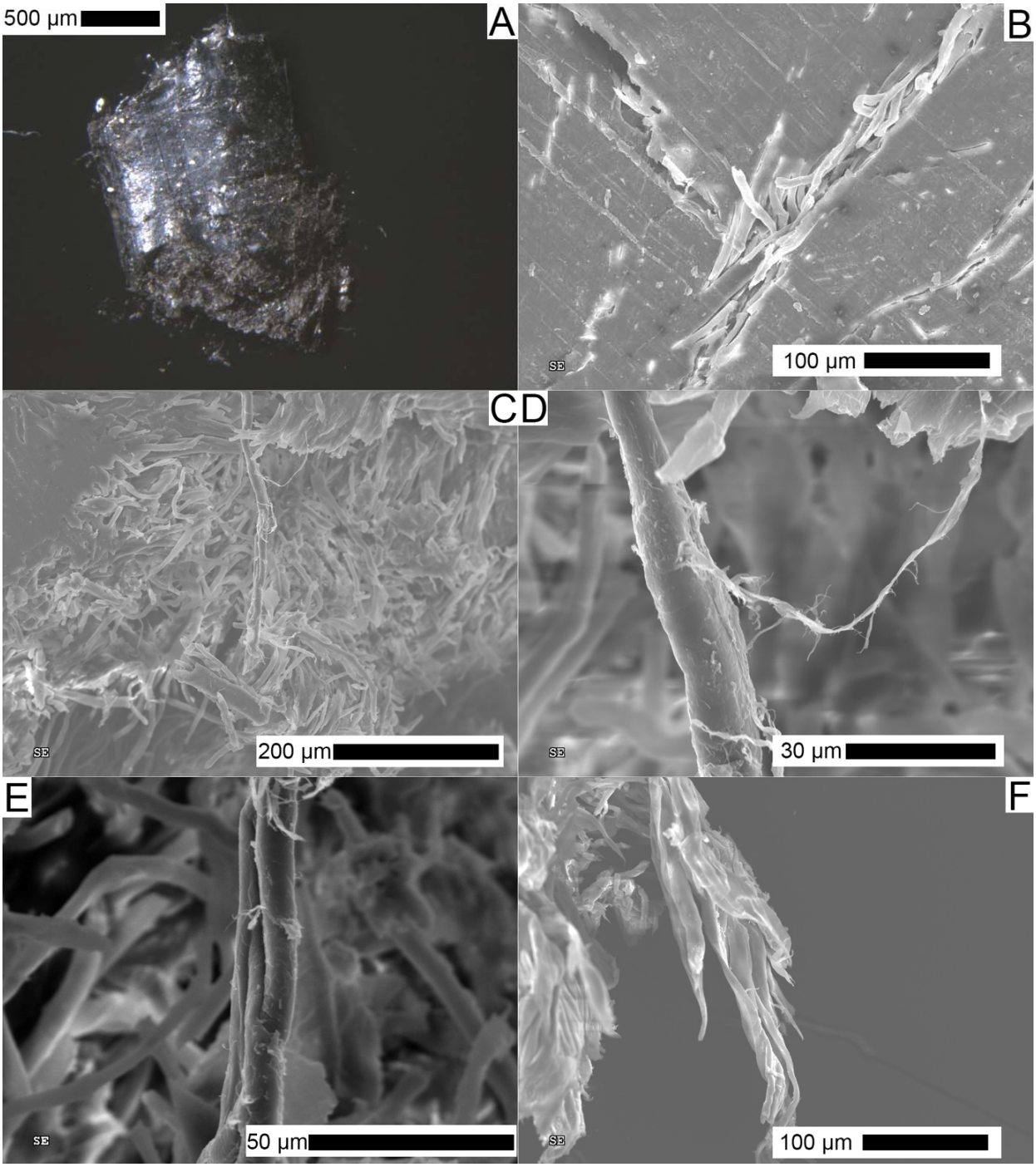

FIG. S24. Structural features of moderately matured decayed iridescent feather. A, under light microscopy, and B–F, SEM.

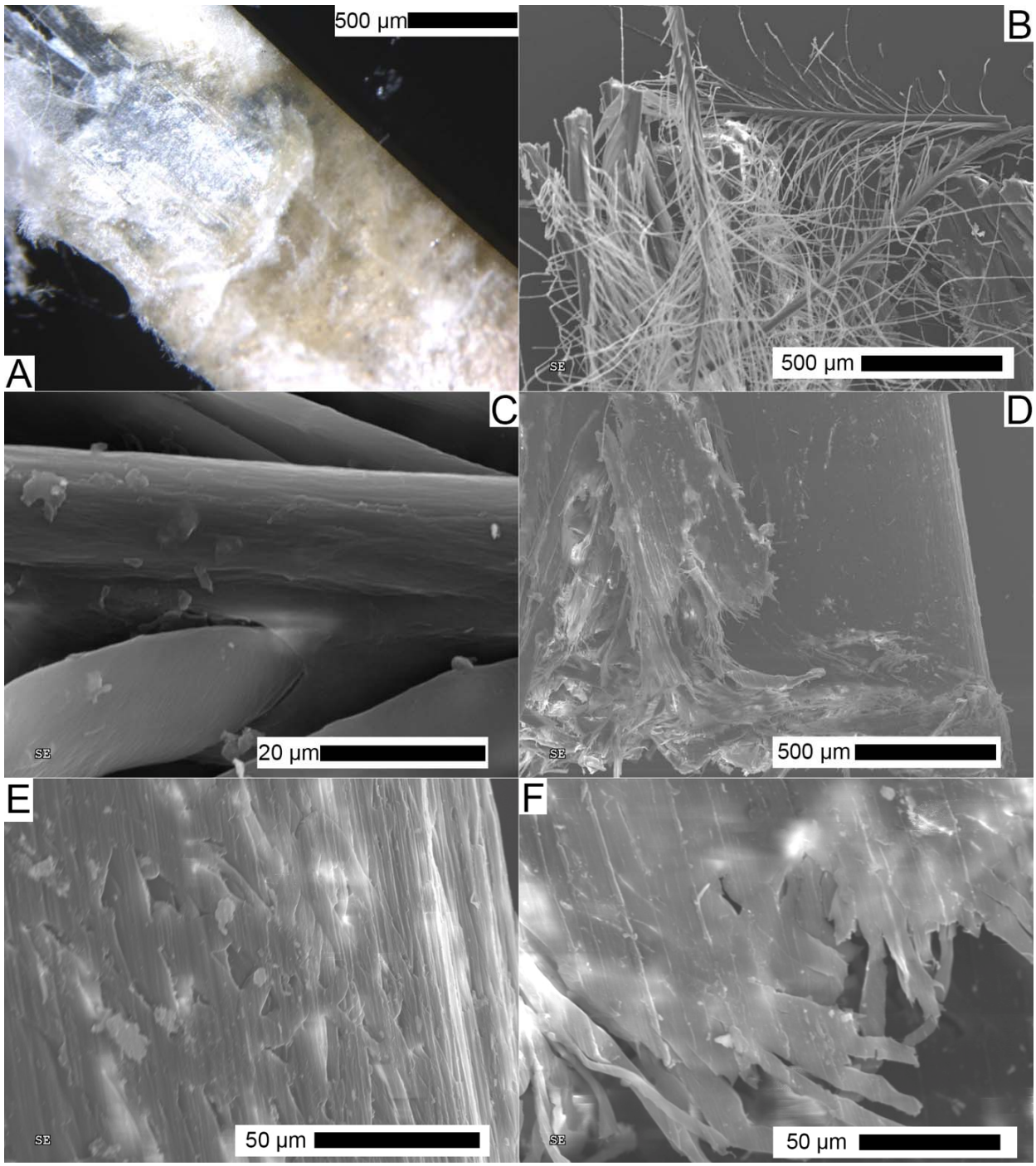

FIG. S25. Structural features of moderately matured white feather. A, under light microscopy, and B–F, SEM. A, calamus. B–C, plumulaceous barbs and barbules. D–F, calamus surface.

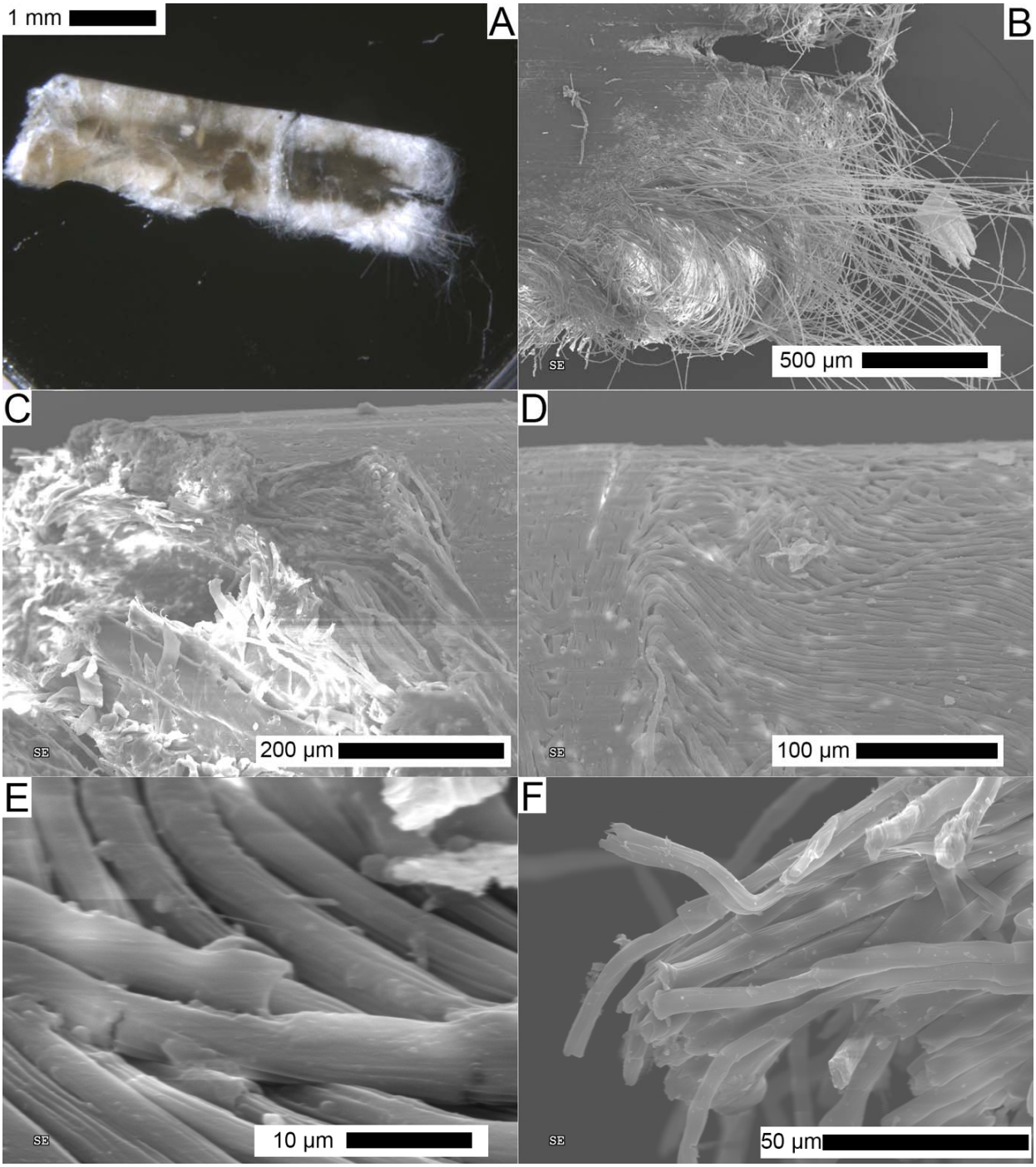

FIG. S26. Structural features of moderately matured decayed white feather. A, under light microscopy, and B–F, SEM. B, plumulaceous barbules and rachis. C–F, calamus.

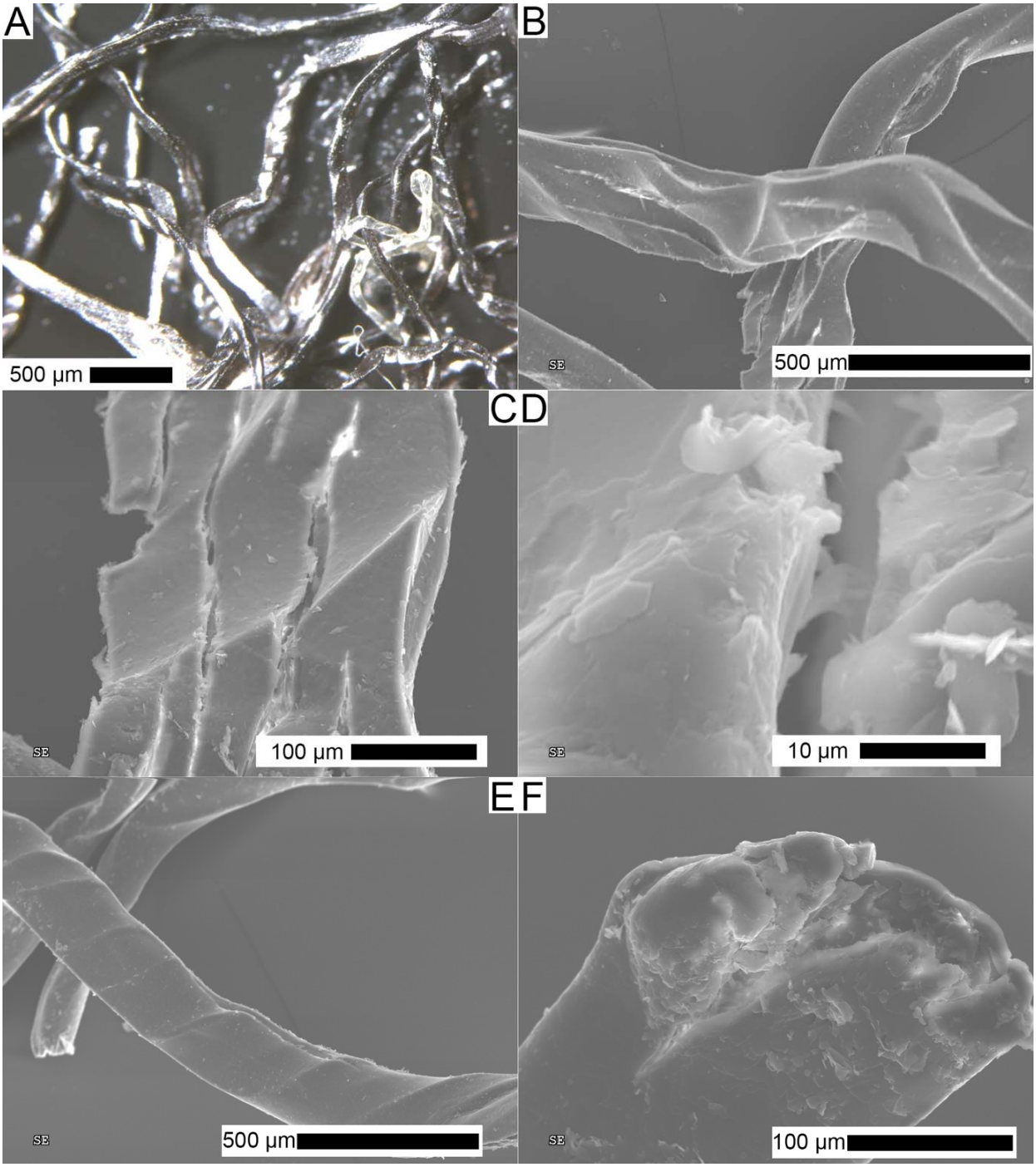

FIG. S27. Structural features of moderately matured horse hair. A, under light microscopy, and B–F, SEM. A–E, surface. F, cross section.

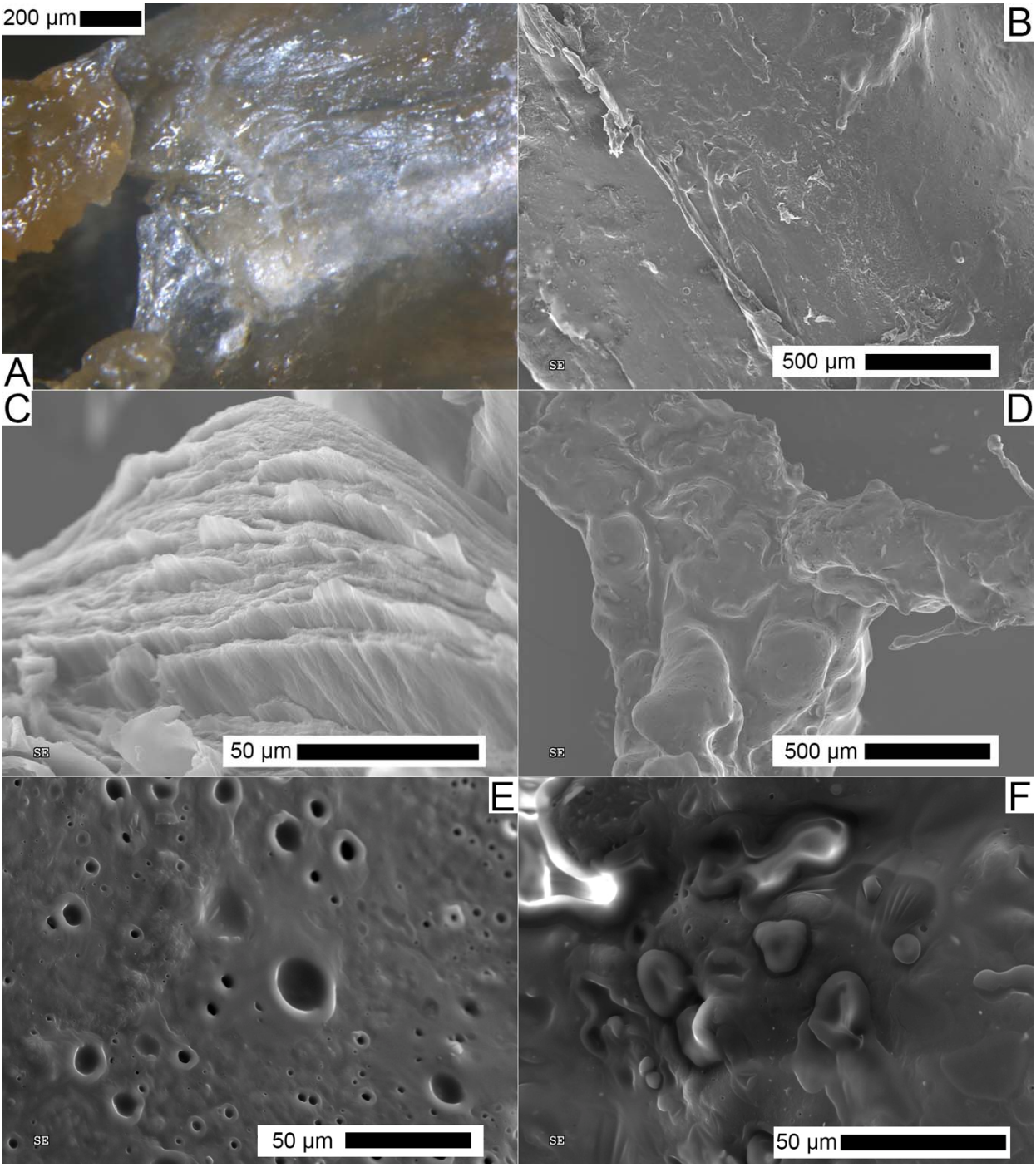

FIG. S28. Structural features of moderately matured avian reticulate scales. A, under light microscopy, and B–F, SEM. B–C, harder remnants. D–F, softer remnants.

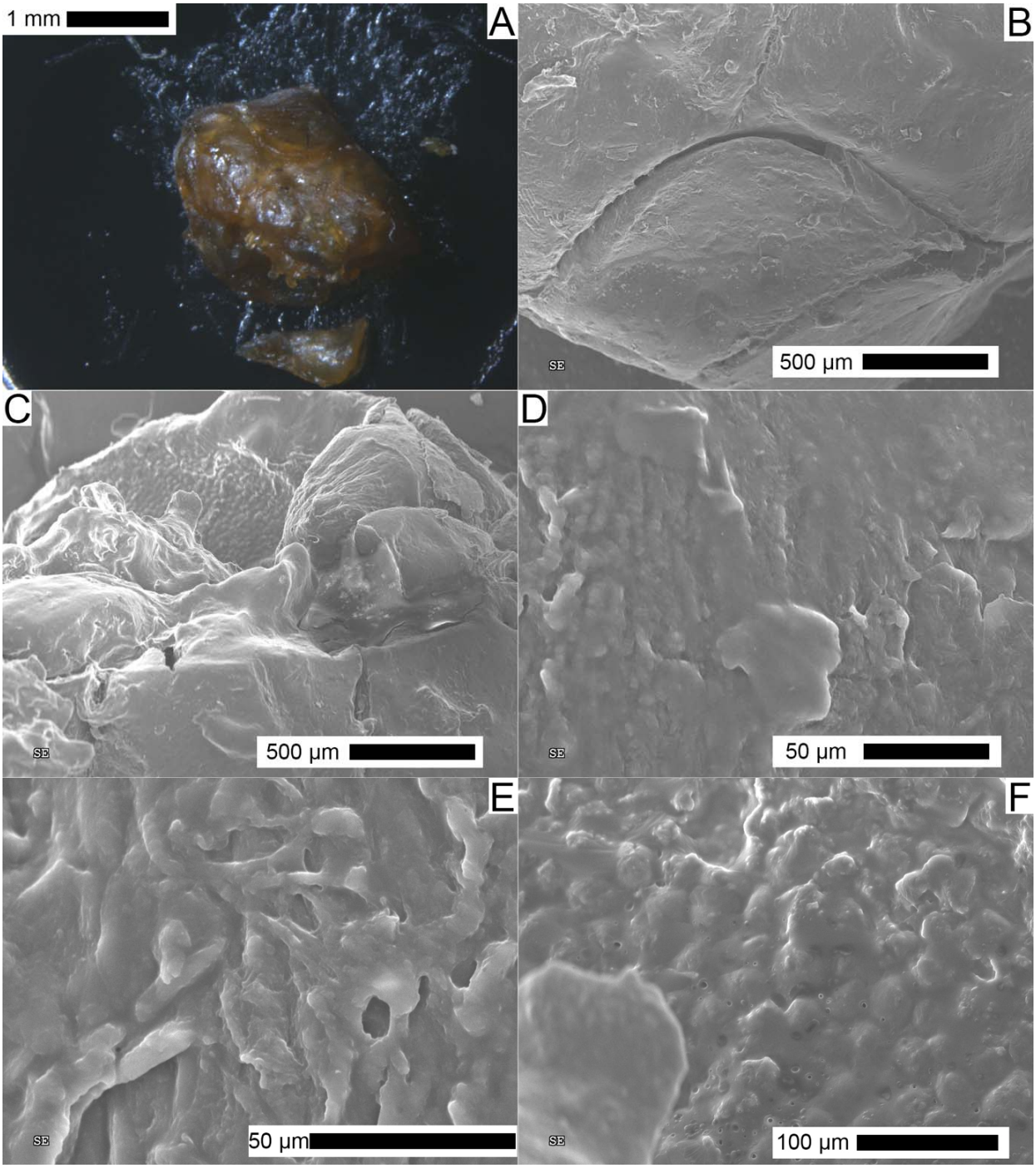

FIG. S29. Structural features of moderately matured avian scutate scales. A, under light microscopy, and B–F, SEM.

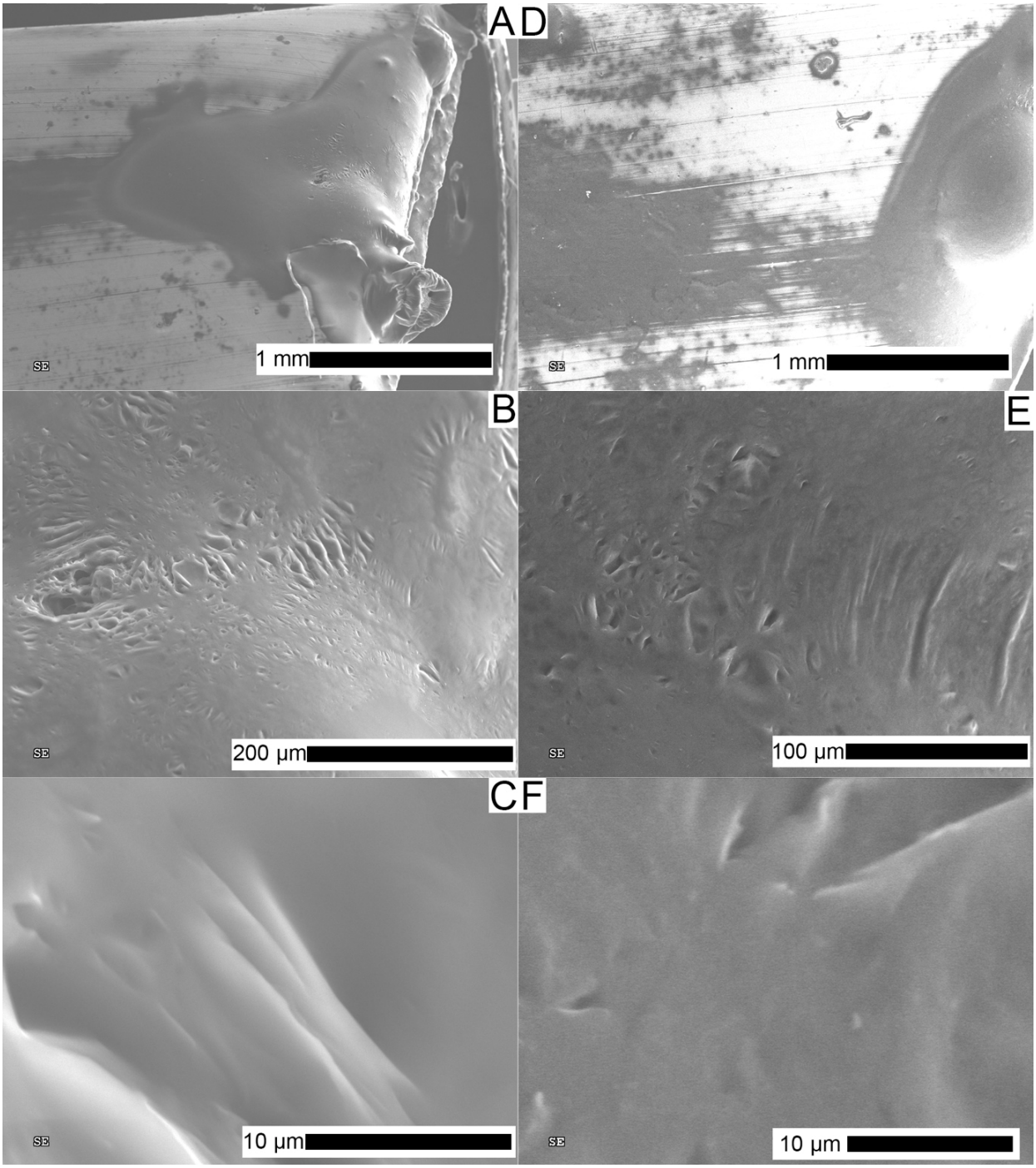

FIG. S30. SEM images of structural features of highly matured feather ‘goo’. A–C, ‘goo’ produced from dark feathers. D–F, ‘goo’ produced from white feathers. A, D, ‘goo’ can be seen to have extruded onto the surface of the capsule.

EXTENDED DISCUSSION

Structural analysis

Fresh samples. The morphology and ultrastructure of the various fresh keratinous structures match previous descriptions in the literature (e.g. Lucas & Stettenheim 1972), as expected. However, there are some interesting comparisons.

The bristles of the turkey beards have a habit of fraying or splitting at their ends when cut, unlike feathers and horse hair. This might be due to the unique keratin makeup of bristles – a combination of feather-type and avian scale-type ϕ-keratins – or their internal structure – an irregularly-shaped and often solid cross-section, unlike feathers, with more organized internal keratin than horse hair. It was also interesting that the flaking on the outer surface of the bristle was more reminiscent of α-keratin horse hair than ϕ-keratin in feathers. There seem to be significant changes in the bristles due to ontogeny, with juvenile bristles being more irregular in cross-sectional shape than adult bristles. Cross sections of the moderately matured adult bristles show that some have hollow centers, as has been previously reported (Schorger 1957). It appears that cross section morphology is highly distinct between feathers, turkey beards, scales, and mammalian hair. Fossil integumentary filaments in dinosaurs have been described as hollow in different instances using conflicting and often weak evidence – some citing dark banding on the edges (Chen *et al.* 1998) and others citing dark banding in the center (Mayr *et al.* 2002). However, Mayr *et al.* (2016) later clarified that these are remnants of melanin preservation and the laser stimulated fluorescence reveals internal structures of *Psittacosaurus* bristles consistent with the interpretation of an internal pith meaning that dark banding patterns in fossil filaments are possibly simply indicating melanin preservation rather than internal structure. Given the implications for how we interpret growth in these integumentary structures, morphology of the cross sections of primitive integumentary structures could be useful if this information can survive fossilization (see Mayer *et al.* 2016).

Feather barbules can show a good amount of variation, and most intriguingly, can have a unique morphology in an iridescent portion of a feather. Plumulaceous barbule nodes in this study either had ring-like morphology or had a multi-pronged morphology. These observations are largely consistent with those reported in the literature (Lucas & Stettenheim 1972). Some rachis cross sections lack columnar organization of the outer cortex and cross-sectional shape can vary in irregularity.

Decayed samples. Bacteria and fungi are known to secrete metalloenzymes utilizing various metal ions that deposit onto the keratin surface (Gupta & Ramnani 2006). The most surprising result from the feather decay experiment was that melanized feathers (black and iridescent) decayed much faster than the non-melanized feathers (white). In fact, the white feathers were most similar to the control feathers in terms of their degradation. The overall morphology of the white feathers was preserved and even the ultrastructural features of the keratin appear little affected by decay contrary to previous studies (Gunderson *et al.* 2008), although the hair-like structures on the surface of one portion of the rachis are peculiar, and may represent early stages of keratin decay. It is possible that, regardless of the potential effect of melanin on microbial decay resistance, other factors might be more important in feather decay such as the structure of the feather, the amount of calcium phosphate deposition within the keratin, or surface lipids. More work is needed to determine the relative importance of feather characteristics in providing decay resistance.

The contribution of melanin to decay resistance cannot be outright rejected since the surviving components of the decayed black feather are mostly melanized. The lighter portions fringing the barbs and the rachis (which was not always fully pigmented) seem to be less

represented in the sample. However, a similar pattern of rachis loss and barb/barbule retention was seen in the decayed iridescent feather, and these were melanized throughout (including their rachises) implying that the structure of different feather parts has a greater contribution to decay resistance than melanin. The white flecks in the decayed black feather 'lint' are potentially the remnants containing high amounts of calcium phosphate from the rachis or calamus.

The connection between the barbules and barbs was preserved more readily than the connection between the barbs and rachis in the decayed black and iridescent feathers, and in the decayed black feather, these remnants of barbs and barbules also show semi-fusion into a mass. Sausage-shaped eumelanosomes from the decayed black and iridescent feathers are apparent. This is likely due to breakdown of the rachis keratin, which could be seen fraying in the sample of decayed iridescent feathers. This breakdown of the rachis also reveals the medulloid cells of the pith, which sometimes appear collapsed (possibly as a result of the vacuum conditions during SEM). The decayed black and iridescent feathers also both show keratin surfaces with a woven texture, rather than simply breaking apart into smaller pieces.

Matured samples. Even at relatively low temperatures (100°C), maturation had major effects on the morphology and ultrastructure of the integumentary appendages.

Both moderately matured juvenile and moderately matured adult turkey bristles show surface degradation and cross-sectional compression. However, the moderately matured juvenile bristles show extreme curling while the moderately matured adult bristles exhibit simple wrinkling or creasing. The flaking of the epidermis is similar in both ontogenetic stages.

The moderately matured black feather retains the original color range (black with white fringe) better than did the non-matured decayed black feather. Like the non-matured decayed black feather, the moderately matured black feather resulted in a mass of barbs and barbules. While these were semi-fused with highly degraded surfaces in the non-matured decayed black feather, the moderately matured black feather showed no fusion and the barbs and barbules were kinked rather than degrading along the surface of the keratin.

Compared to the non-matured decayed black feather, the moderately matured decayed black feather shows great fusion of the barbs and barbules such that only a few can be identified among the solid mass. Some of the flaking seen in the keratin surface of the non-matured decayed black feather appears to be intensified into the granulated texture of some regions on the moderately matured decayed black feather.

Like the non-matured decayed iridescent feather, the moderately matured iridescent feather consists of a mass of barbs and barbules. Both retain some degree of iridescence, although this is reduced in the moderately matured sample. Similar to the moderately matured vs. non-matured decayed black feather, the moderately matured iridescent feather shows a loss of overall feather morphology, but the keratin surface does not appear as degraded as that of the non-matured decayed iridescent feather.

The moderately matured decayed iridescent feather has turned into a pellet similar to that of the moderately matured decayed black feather. Most of the features still present in the non-matured decayed iridescent feather are lost in the moderately matured decayed iridescent feather, although barbules attached to degraded barbs can still be made out. Unlike the woven texture seen in the non-matured decayed iridescent feather, the keratin of what was presumably once the rachis is peeling into large strips or strands in the matured decayed iridescent feather.

The moderately matured white feather shows degradation of the overall feather morphology and also shows the peeling off of large strips or strands on its rachis/calamus. It is

hard to compare maturation to decay in this instance since the white feather decayed at such a slow rate in the experiment, resulting in little signs of degradation.

The moderately matured decayed white feather shows similar loss of overall feather morphology to the moderately matured white feather, but effect on the rachis/calamus keratin is more extreme. Instead of simply peeling off into strips or strands, an organized mesh of filaments is exposed. A previous study used microbial degradation of the rachis keratin to better study the filamentous hierarchy within (Lingham-Soliar *et al.* 2009). The reported filaments, similar to those observed here, are the thickest of any keratin filament (6 μm), extend along the axis of the rachis with a small outer circumferential layer, and have thickened nodes staggering between adjacent filaments along two and three dimensions. In that study and here, filaments appear almost identical to plumulaceous barbules – a fact that these researchers cite as evidence for an evo-devo model of feather evolution in which barbs fuse together during development to form the rachis, as proposed by Prum & Brush (2002). While the results here support the existence of these filamentous subunits of the rachis, it is interesting that the other researchers observed them through decay alone. Here, they were only apparent in the moderately matured decayed white feather. The peeling off of strands or strips in the moderately matured decayed iridescent and moderately matured white feathers as well as the woven texture seen in the non-matured decayed black and non-matured decayed iridescent feathers might represent early stages of degradation in which these filamentous subunits are not fully exposed.

Although the decay experiments found the more melanized feathers to degrade faster, maturation seemed to show the opposite trend. The greatest morphological and ultrastructural changes as well as the greatest amount of rachis/calamus keratin degradation as a result of maturation occurs in the white feathers. While other factors might be more important in conferring decay resistance to feathers than melanin, melanin might be important in reducing the rate of degradation due to maturation.

In all three feather colors, maturation did not produce identical effects as decay, particularly at the ultrastructural level of the keratin surface. This is reflective of the activity of microbes degrading the keratin surface during decay, while the intense temperature and pressure of maturation can affect the keratin structure as a whole, rather than just at its surface. However, maturation and decay can both break down the overall structure of the feather. Of all samples (excluding those highly matured), the greatest amount of degradation occurred in the moderately matured decayed feathers, as might be expected.

Differences in degradation patterns between moderately matured filaments might relate to their keratin type: helical curling and kinking in the moderately matured horse hair (α-keratin), curling of the moderately matured juvenile turkey bristles (both feather-type and avian scale-type ϕ-keratins), wrinkling and creasing of the moderately matured adult turkey bristles (both feather-type and avian scale-type ϕ-keratins, although their dried nature prior to treatment should be kept in mind), and the kinking of the moderately matured black feather (feather-type ϕ-keratins) were observed. These differences could be useful only if they left some sort of signature in fossils.

Both predominantly black and predominantly white moderately matured crocodile scales show cracking of their outer layer, splitting between the sub-layers of the outer layer, and retention of the rippled ultrastructural surface. While the moderately matured predominantly white scale was slightly discolored, the moderately matured black scale retained its original range of coloration. The internal layer of the scales matured into a soft substance.

Like the moderately matured crocodile scales, the moderately matured avian reticulate scales show harder and softer remnants. The softer remnants, likely derived from the inner layer of the scales, show interesting folded features that come in a range of morphologies.

The moderately matured avian scutate scale does not show as many features as did the moderately matured reticulate scales and the harder and softer portions are more difficult to distinguish in the sample. All of the various scale types in this study matured into pliable masses, although the original outer and inner layers of the scales were more recognizable after maturation in the scales made of non-featherlike β-keratins than those made of ϕ-keratins (the scutate scales).

The rippled ultrastructural surface of the outer layer of fresh and moderately matured crocodile and fresh avian reticulate scales is more complex than the relatively smooth keratin surface of feathers. These scales are made of non-featherlike β-keratin. The scutate scales show a relatively smooth ultrastructural surface, more like feathers (both consisting of ϕ-keratin). Some might take this ultrastructural similarity as further evidence that scutate scales evolved via modification of leg feathers (Zheng et al. 2013). As is the case for the observed differences in degradation patterns in moderately matured filaments described above, even if the rippled texture of scales is an accurate indicator of keratin type, and it survives moderate heat and pressures, the question remains as to whether it can survive the extreme conditions of fossilization.

The ‘goo’ produced from highly matured feathers shows complete degradation of the keratin ultrastructure. Melanosomes cannot be recognized in the ‘goo’ derived from dark feathers, which is surprising considering their widespread presence in fossils (Vinther *et al.* 2008, Vinther 2015). It is possible that melanosomes did survive maturation but became obscured by the ‘goo’.

More importantly, the presence of this ‘goo’ contradicts previous work in which feathers exposed to comparably high temperatures and pressures (200°C/250 bars and 250°C/250 bars) for (reportedly) 24 hours retained the majority of their original morphology (McNamara *et al.* 2013). Repeating the experiments detailed by McNamara *et al.* failed to reproduce their results. Furthermore, retention of feather morphology was not observed here even after a lower temperature maturation of white feathers (200°C/250 bars/24 hours), which also produced a ‘goo’ that leaked out of the tube. Repeating the exact temperatures, pressure, and duration they reported (and in the maturation runs where the samples were lost, similarly using an Ar gas, rather than a cold seal, autoclave) failed to produce results similar to those they report. In their supplemental material, however, McNamara *et al.* state, “Experiments were undertaken at: 200°C, 1 bar; 200°C, 117 bar; 200°C, 250 bar; 200°C, 500 bar; 270°C, 500 bar; 25°C, 500 bar, each for 24 hours. 1 hour experiments were run at 200°C, 250 bar and 250°C, 250 bar”. The results they present were actually from maturation experiments run for 1 hour rather than 24 hours, and the main text of the paper reports an incorrect procedure.

ADDITIONAL SUPPORTING FIGURES AND TABLES

FIG. S32. Dark and white feather types that were highly matured (250°C) into ‘goo’ for analysis.

Sample	Number of samples loaded	Did the capsule gain weight after autoclaving?	Was the capsule crushed after autoclaving?
Crocodile scale – mostly black	Small portion of 1 scale	No	Yes
Crocodile scale – mostly white	Small portion of 1 scale	No	Yes
Juvenile turkey beard	Multiple bristles with attached epidermis	No	Yes
Adult turkey beard	Multiple cut bristles with attached epidermis	No	No
Iridescent feather	Tips of 2 feathers	No	Yes
Decayed iridescent feather	Capsule half full	Yes	Yes
Decayed white feather	1 feather; Cut in half	No	Yes
Decayed black feather	Capsule half full	No	Yes
Horse hair	Multiple cut hairs	No	Yes
Black feather	$2^{2}/_{3}$ feathers; Cut	No	No
Avian scutate scale	1 scale	No	Yes
Avian reticulate scale	Multiple scales with attached epidermis	No	Yes
White feather	2 feathers; Cut	No	Yes
‘Goo’ from dark feathers	1 feather; Cut	No	Yes
‘Goo’ from white feathers	2 feathers; Cut	No	Yes

Table S1. Autoclave capsule information.

Decayed feathers

FIG. S34. Decayed white feathers. A–B, in Pyrex jars and salt/microbial broth. C, after removing from broth.

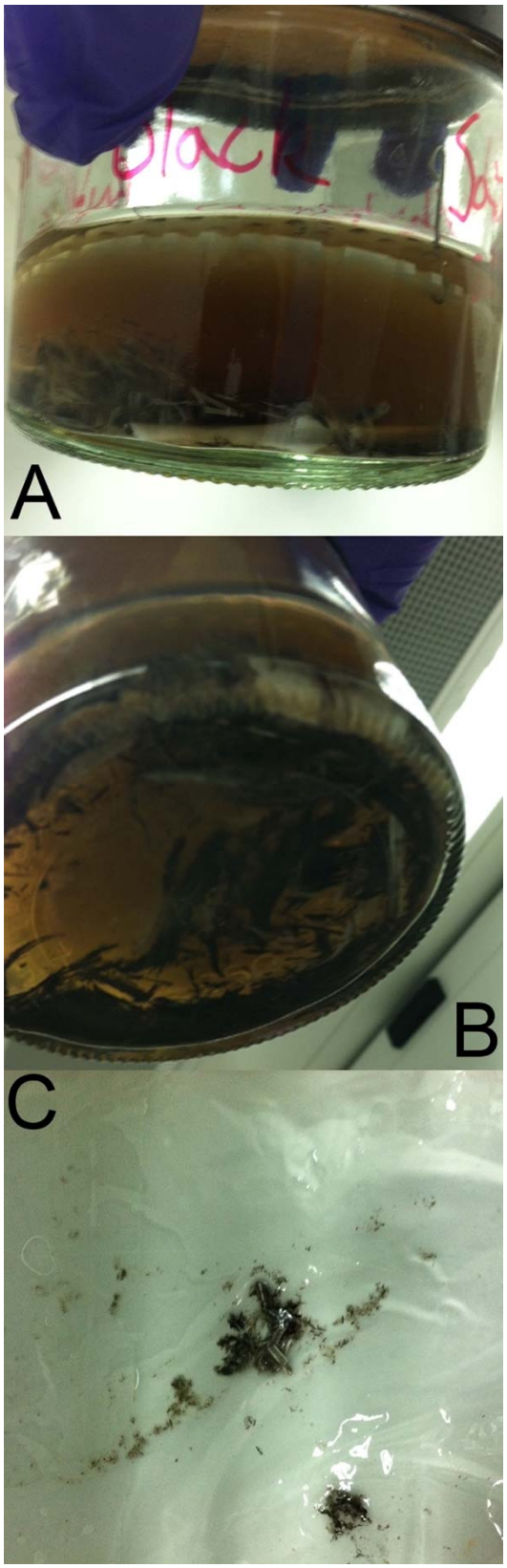

FIG. S35. Decayed black feathers. A–B, in Pyrex jars and salt/microbial broth. C, after removing from broth.

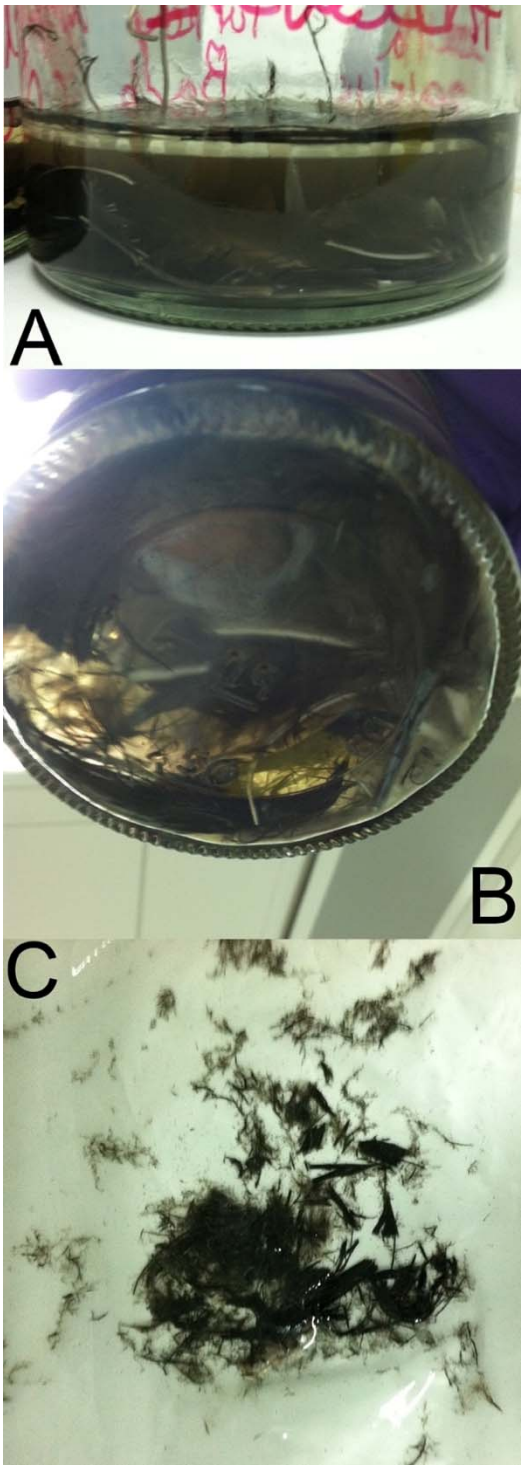

FIG. S36. Decayed iridescent feathers. A–B, in Pyrex jars and salt/microbial broth. C, after removing from broth.

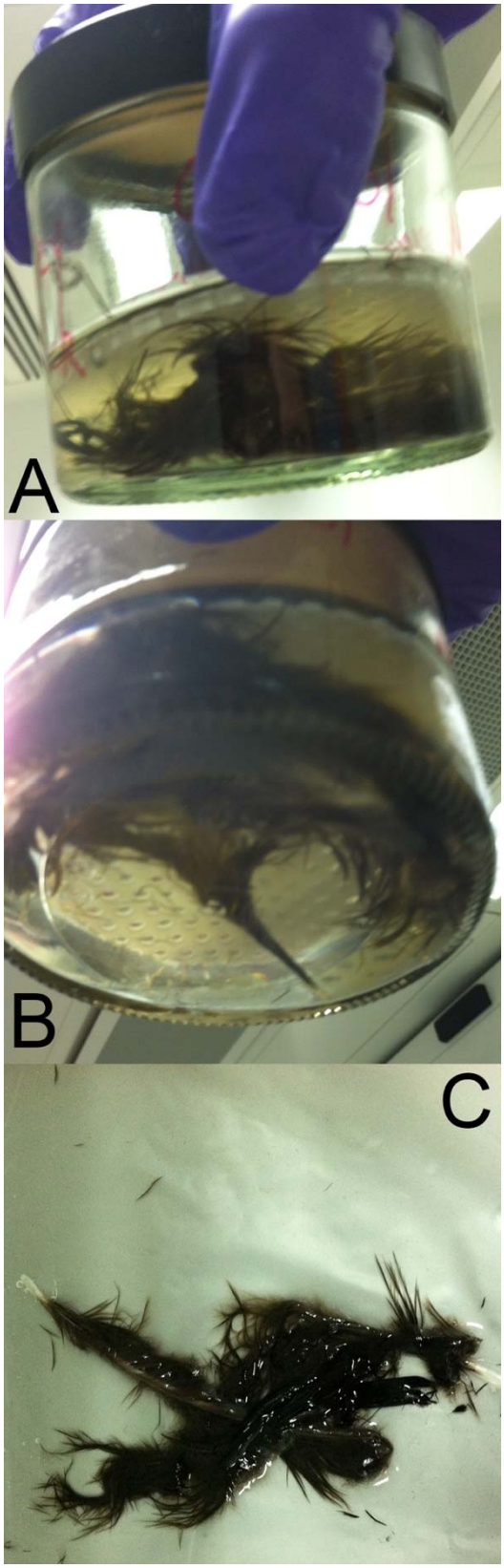

FIG. S37. Decayed control feathers. A–B, in Pyrex jars and salt/microbial broth. C, after removing from broth.

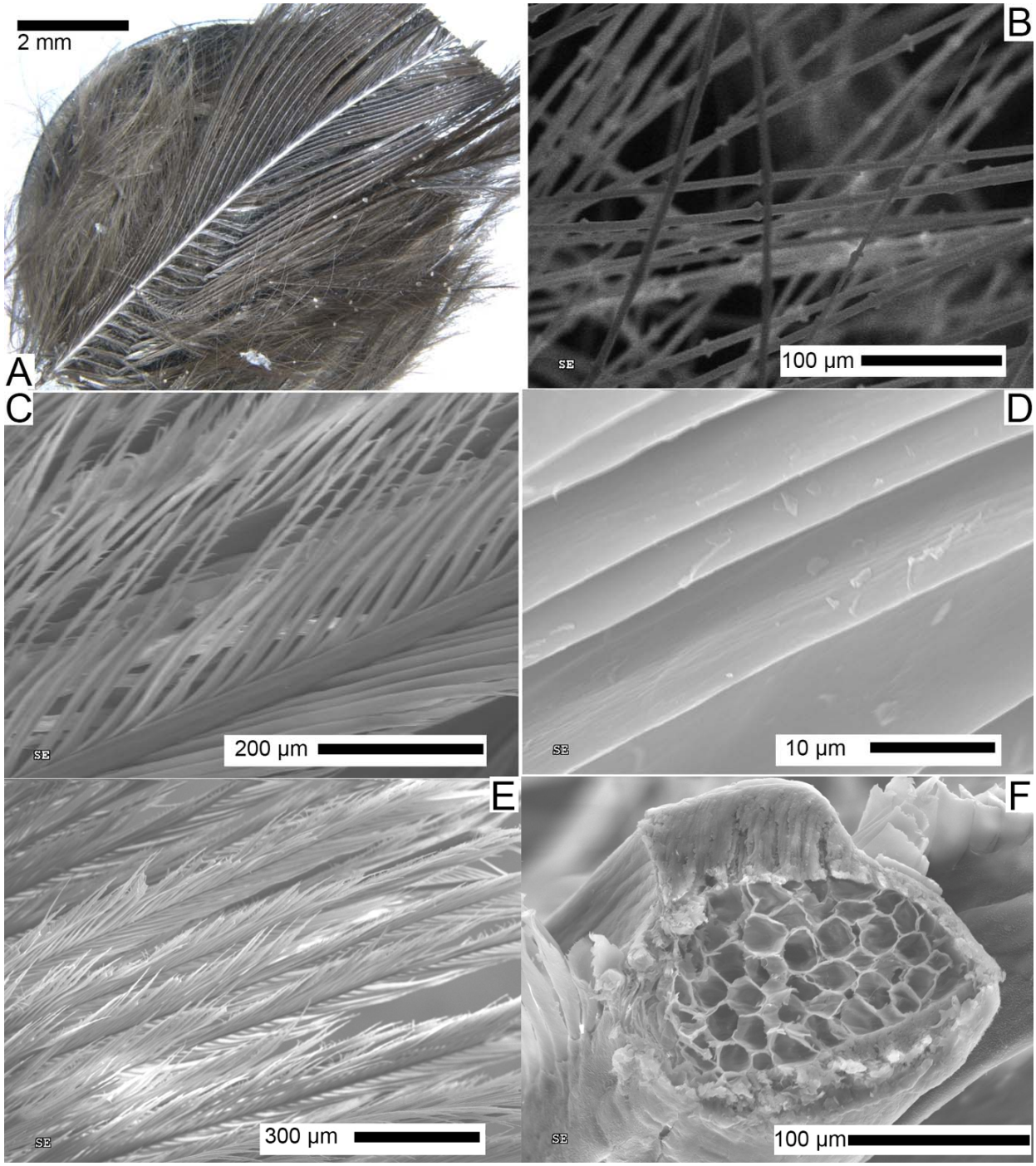

FIG. S38. Structural features of decayed control feathers rinsed with ethanol after decay treatment. A, under light microscopy, and B–F, SEM. B, plumulaceous barbs. C–E, pennaceous barbs and barbules. F, cross section of rachis.

LITERATURE CITED

Chen, P. J., Dong, Z. M., and Zhen, S. N. 1998. An exceptionally well-preserved theropod dinosaur from the Yixian Formation of China. *Nature*, **391**, 147–152.

Gunderson, A. R., Frame, A. M., Swaddle, J. P., and Forsyth, M. H. 2008. Resistance of melanized feathers to bacterial degradation: is it really so black and white?. *Journal of Avian Biology*, **39**, 539–545.

Gupta, R. and Ramnani, P. 2006. Microbial keratinases and their prospective applications: an overview. *Applied Microbiology and Biotechnology*, **70**, 21–33.

Lingham-Soliar, T., Bonser, R. H., and Wesley-Smith, J. 2009. Selective biodegradation of keratin matrix in feather rachis reveals classic bioengineering. *Proceedings of the Royal Society of London B: Biological Sciences*, **277**, 1161–1168.

Lucas, A. M. and Stettenheim, P. R. 1972. *Avian Anatomy Integument. Part 1*. U. S. Government Printing Office, Washington, D. C.

Mayr, G., Peters, S. D., Plodowski, G., and Vogel, O. 2002. Bristle-like integumentary structures at the tail of the horned dinosaur *Psittacosaurus*. *Naturwissenschaften*, **89**, 361–365.

Mayr, G., Pittman, M., Saitta, E., Kaye, T. G., and Vinther, J. 2016. Structure and homology of *Psittacosaurus* tail bristles. *Palaeontology*. doi:10.1111/pala.12257.

McNamara, M.E., Briggs, D. E. G., Orr, P. J., Field, D. J., and Wang, Z. 2013. Experimental maturation of feathers: implications for reconstructions of fossil feather colour. *Biology Letters*, **9**, 20130184.

Prum, R. O. and Brush, A. H. 2002. The evolutionary origin and diversification of feathers. *The Quarterly Review of Biology*, **77**, 261–295.

Schorger, A. W. 1957. The beard of the wild turkey. *The Auk*, **74**, 441–446.

Vinther, J. 2015. A guide to the field of palaeo colour. *BioEssays*, **37**, 643–656.

Vinther, J., Briggs, D. E. G., Prum, R. O., and Saranathan, V. 2008. The colour of fossil feathers. *Biology Letters*, **4**, 522–525.

Zheng, X., Zhou, Z., Wang, X., Zhang, F., Zhang, X., Wang, Y., Wei, G., Wang, S., and Xu, X. 2013. Hind wings in basal birds and the evolution of leg feathers. *Science*, **339**, 1309–1312.